

THESIS

DEVELOPMENT OF AN OVINE CARDIAC MODEL FOR THE MODIFIED BLALOCK-
THOMAS-TAUSSIG SHUNT

Submitted by

Margaret Lucinda Chu

Department of Clinical Sciences

In partial fulfillment of the requirements

For the degree of Master of Science

Colorado State University

Fort Collins, Colorado

Spring 2023

Master's Committee:

Advisor: Eric Monnet

Sarah Marvel
Elissa Randall

Copyright by Margaret Lucinda Chu 2023

All Rights Reserved

ABSTRACT

DEVELOPMENT OF AN OVINE CARDIAC MODEL FOR THE MODIFIED BLALOCK- THOMAS-TAUSSIG SHUNT

This pilot study aimed to better describe the ovine thoracic vascular anatomy, to develop a model for placement of a modified Blalock-Thomas-Taussig (BT) shunt in sheep, and to evaluate whether hyaluronan-treated grafts would have decreased thrombosis and adherence compared to traditional polytetrafluoroethylene (PTFE) grafts. Ovine thoracic vasculature follows the pattern of a bovine aortic arch and branching of arterial vascular does not occur until the thoracic inlet. A prominent left azygos vein and ligamentum arteriosum are also present. Placement of a modified BT-shunt was possible in sheep and did appear to lead to some long-term changes in cardiac values. Hyaluronan-treated shunts were subjectively less adherent with incomplete thrombosis occurring in the subjects. Further research is needed to better evaluate the latter two aims of this project.

ACKNOWLEDGEMENTS

I would like to acknowledge the contributions of the PSRL team to the surgical set up, management of the sheep used in this project, and all of the logistics needed for pre and post-surgical research. All below would not be possible without their hard work and care.

Acknowledgement is also due to Holly Stewart, CSU Animal Care, and the CSU Livestock hospital for their invaluable post-operative care as well as to Brian Scansen, Alex Ohlendorf, and Ariel Brody for the images reviewed in this project. And, of course, Eric Monnet for his supervision and advice as well as Sarah Marvel and Elissa Randall for their support.

TABLE OF CONTENTS

ABSTRACT	ii
ACKNOWLEDGEMENTS.....	iii
CHAPTERS	
I. INTRODUCTION.....	1
Statement of Problem.....	2
Hypothesis.....	2
II. REVIEW OF LITERATURE	3
Cyanotic Congenital Heart Defects.....	3
Palliative Shunt Procedures.....	15
Ovine Cardiac Model.....	18
Cardiac Work.....	19
III. ANATOMICAL STUDY.....	22
Methods.....	22
Results.....	22
IV. CADAVERIC PROOF OF CONCEPT.....	26
Methods.....	26
Results.....	27
V. PILOT LIVE SHEEP STUDY.....	29
Methods.....	29
Results.....	33
VI. DISCUSSION, CONCLUSIONS AND RECOMMENDATIONS.....	42
Discussion.....	42
Conclusions.....	45
Recommendations for Further Study.....	45
REFERENCES	47
LIST OF ABBREVIATIONS.....	53

Chapter I

Introduction

Congenital heart diseases or defects (CHD) are a common pediatric problem affecting 1.35 million births globally each year at an estimated incidence of 8 to 9.1 in every live 1000 births (Bernier, Stefanescu, Samoukovic, & Tchervenkov, 2010; Van Der Linde et al., 2011). While infant mortality has improved globally with the advent of open-heart surgery and transcatheter procedures, it is still estimated that over 250,000 individuals died from a CHD in 2017 (Zimmerman et al., 2020). However, as >90% of children born with CHD now survive to adulthood, this has led to a growing population of adults that require treatment for a spectrum of diseases and sequelae from advanced surgical repairs (Sommer, Hijazi, & Rhodes, 2008b).

Critical CHD are defects where repair is needed to prevent death or disability in the first year of life. This is particularly true for cyanotic heart defects, which can comprise some of the most complex CHD. Whenever possible, definitive treatment for critical CHD is pursued as soon as possible to allow infants to grow with as few side-effects as possible. However, there are circumstances where definitive treatment may not be physiologically or anatomically possible immediately but the patient is symptomatic, thus requiring a palliative treatment. Therefore, it becomes continually more important to improve and better understand the cardiac physiology of palliative procedures like the Blalock-Thomas-Taussig (BT) shunt for our growing surviving CHD population as well as for our increasing number of veterinary patients with owners interested in pursuing treatment for CHD.

Statement of Problem

BT shunts lead to short- and long-term changes to cardiac physiology that are relevant to the management of congenital heart diseases. Use of an ovine model can help elucidate some of these changes as well as help determine whether different shunt materials may allow for more successful shunt placement.

Hypotheses

1. There would be cardiac remodeling secondary to BT shunt placement in the ovine model.
2. BT shunts treated with hyaluronan would have decreased thrombosis and adherence when compared to normal polytetrafluoroethylene (PTFE) shunts.

Chapter II

Review of Literature

Cyanotic Congenital Heart Defects

Cyanotic CHD are defects that results in deoxygenated blood entering systemic circulation, thus making the infant appear blue or cyanotic. Chronic hypoxemia can result in clubbing of the hands and feet, erythropoietin release from the kidneys to increase red blood cell production and subsequent polycythemia, coagulation abnormalities, and hyperuricemia. Hypercyanotic or tet spells can also occur, generally following increased infant activity, and present as convulsions, limpness or syncope (Rao, 2019). Cyanotic heart diseases are some of the most complex congenital heart defects documented, and most require some procedure to allow the patient to survive.

There are many CHD that are documented to cause cyanosis: truncus arteriosus, transposition of the great arteries, tricuspid atresia, tetralogy of Fallot, total anomalous pulmonary venous connection, Ebstein anomaly, hypoplastic left heart syndrome, pulmonary atresia with intact ventricular septal defect, double-outlet right ventricle, double-inlet left ventricle, and univentricular hearts. The first five or the "5 Ts" are the most well documented and are thus reviewed regarding nomenclature, embryology, pathophysiology, repair, and incidence in veterinary medicine.

I. Persistent truncus arteriosus

Persistent truncus arteriosus, truncus arteriosus communis, or common arterial trunk describes CHD with a single major vessel as the outlet tract of the heart. The vessel gives rise to

the aorta, pulmonary trunk or arteries, and coronary arteries. Most commonly, a ventricular septal defect (VSD) is present as well. This defect occurs when the embryological truncus arteriosus and, occasionally, bulbus cordis fail to divide into the aorta and the pulmonary trunk as well as the semilunar valves, respectively. However, no specific cause has been identified (Ezon, Goldberg, & Kyle, 2015; Jacobs & Anderson, 2012; Rao, 2019).

Multiple nomenclature systems have been described for persistent truncus arteriosus, including some by Collett and Edwards, Van Praagh and Van Praagh, and the Congenital Heart Surgery Nomenclature and Database Project through Russell et al. In the Collett and Edwards classification scheme, pulmonary vasculature is used to differentiate:

type I: a single, confluent pulmonary segment arises from a common arterial trunk, then branches

type II: more than 1 pulmonary artery arises adjacent to each other from the common trunk

type III: more than 1 pulmonary artery arises non-adjacent to each other from the common trunk

type IV: pulmonary arteries arise separately not from the common trunk.

Collett and Edwards type IV is now generally described as pulmonary atresia with VSD with major aortopulmonary collateral arteries (MAPCAs) rather than persistent truncus arteriosus (Collett & Edwards, 1949; Kochi, Sugimoto, Kawamoto, Inoue, & Machida, 2021).

The Van Praagh classification scheme divides truncus arteriosus communis into 2 larger groups with modifiers A and B. Group A refers to patients with a concurrent VSD. Patients in group B do not have a concurrent VSD, but this is significantly less common.

type A1: an aortopulmonary septal remnant is present so that a short segment of main pulmonary artery arises from the common arterial trunk

type A2: no aortopulmonary septal remnant is present so that the branch pulmonary arteries are arising from the common arterial trunk

type A3: one of the pulmonary arteries does not arise from the common arterial trunk, but at least one pulmonary artery does arise from the common arterial trunk

type A4: an interrupted aortic arch is present

Van Praagh requires that at least one of the pulmonary arteries must arise from the intrapericardial space to be considered persistent truncus arteriosus; thus, Collett and Edwards type IV would not be considered as truncus arteriosus communis in the Van Praagh classification scheme (Van Praagh, 1976).

Finally, the last approach is to categorize common arterial trunk as aortic or pulmonary dominant, based on the morphology of the common trunk being most characteristic of which "normal" vessel. Aortic dominant trunks supply the brachiocephalic vessels while pulmonary dominant trunks exhibit features similar to aortic coarctation, interrupted aortic arch, or hypoplastic aortic arch (Russell et al., 2011).

Cyanosis occurs in persistent truncus arteriosus because of the mixing of oxygenated and deoxygenated blood in the common outlet. This partially deoxygenated blood is then outputted into the systemic circulation. Presence of a VSD allows further mixing of oxygenated and deoxygenated blood. Shortly after birth, pulmonary vascular resistance decreases, which leads to over-circulation of the lungs from the common trunk and left-sided congestive heart failure. The combination of these pathologies leads infants to become clinical very quickly, and infants are typically diagnosed in the few days following birth.

Surgical repair is typically performed in infancy. Repair is pursued as soon as 10 days following control of congestive heart failure (CHD), if present. A single-stage procedure under cardiopulmonary bypass consists of VSD closure (if present), separation of the pulmonary artery or arteries from the truncus and attachment to the right ventricle, and closure of the defect in the truncus made from removing the pulmonary artery or arteries (Rao, 2019). For Van Praagh type A4 or pulmonary dominant trunks, addressing the aortic interruption and closure of a patent ductus arteriosus is also needed (Talwar, Siddharth, Gupta, Bhoje, & Choudhary, 2019). Staged repair is typically no longer practiced.

Although rare clinical cases, various case reports of persistent truncus arteriosus have been published in veterinary medicine. Case reports exist for species such as the domestic cat, dog, horse, alpaca, cattle as well as Sumatran orangutan and Eastern Black rhinoceros (Chuzel et al., 2007; Jesty, Wilkins, Palmer, & Reef, 2007; Kochi et al., 2021; Kurosawa, Gunasekaran, Sanders, & Carr, 2016; Meister et al., 2022; Monné Rodríguez, Chantrey, Unwin, & Verin, 2017; Schwarzwald, Gerspach, Glaus, Scharf, & Jenni, 2003; Serres, Chetboul, Sampedrano, Gouni, & Pouchelon, 2009; Stephen, Abbott, Middleton, & Clarke, 2000). Most cases in veterinary medicine are classified according to Collett and Edwards and are aortic dominant. Most cases are definitively diagnosed on postmortem examination. The role of computed tomography angiography (CTA) has been documented to assist with antemortem diagnosis (Markovic, Scansen, & Potter, 2017).

II. Transposition of the great arteries

Transposition of the great arteries (d-TGA) occurs when the aortic root is anteriorly and dextropositioned, allowing the aorta to arise from the morphologic right ventricle and the

pulmonary artery from the morphologic left ventricle. The pulmonary valve and mitral valve are in fibrous continuity. This results in 2 independent, parallel circuits, where the systemic and pulmonary circulation do not mix. It is thought to occur due to a failure of the normal clockwise rotation of the aorta to the left ventricle or due to a defect in spiraling of the aorto-pulmonary septum (Unolt et al., 2013). TGA can also occur with dextrocardia, resulting in a mirror image of d-TGA (Ezon et al., 2015).

d-TGA without additional heart defects results in cyanosis, as the 2 parallel circuits do not allow additional oxygenated blood to enter the systemic circulation; the patient quickly uses the available systemic oxygenated blood for cellular metabolism. d-TGA is reliant on the presence of additional shunts such as a patent foramen ovale (PFO) or patent ductus arteriosus (PDA) for the patient to survive (Sommer, Hijazi, & Rhodes, 2008a). Congenitally corrected TGA or l-TGA refers to a L-looped heart that has inverted atrioventricular and ventriculoarterial connections, which then does not create two independent, parallel circuits. These patients, if no additional abnormalities are present, are not cyanotic but eventually have myocardial failure due to the morphological right ventricle being responsible for systemic circulation.

Management of d-TGA is divided into 3 groups: TGA with intact ventricular septum, TGA with VSD, and TGA with VSD and pulmonary stenosis (PS). For the first 2 groups, if adequate mixing is available from PFO or PDA, no immediate intervention is initiated until Jatene arterial switch and LeCompte maneuver with closure of VSD, as appropriate, are performed at about 1 week of life. For patients that do not have adequate mixing, bedside balloon atrial septostomy is performed to allow for greater atrial mixing until definitive treatment can be pursued. If the left ventricle is not appropriately conditioned to support systemic circulation, pulmonary artery banding can be performed to train the left ventricle to support systemic

pressures. For patients with PS in addition to d-TGA and VSD, hypoxemia may be more severe, and initial modified BT shunt and/or balloon pulmonary valvuloplasty are performed to improve the patient until definitive surgery. Rastelli repair has better results for these patients when performed at 1 - 2 years of age (Rao, 2019). l-TGA can be asymptomatic early in life until right ventricular failure; thus, treatment can involve Jatene arterial switch to have the left ventricle support systemic circulation as appropriate or later in life heart transplant (Sommer et al., 2008a).

Most reports of TGA in veterinary medicine involve large animals, likely due to the level of immediate post-natal care offered. TGA with VSD had be described in the horse and cattle (Grünberg, van Bruggen, Eisenberg, Weerts, & Wolfe, 2011; McClure, Gaber, Watters, & Qualls, 1983; Sleeper & Palmer, 2005; Zamora, Vitums, Nyrop, & Sande, 1989). It has also been reported in a kitten with a VSD (Straw, Aronson, & McCaw, 1985). A report of a dog with d-TGA and double-outlet right ventricle (DORV) has been reported (Koo, Leblanc, Scollan, & Sisson, 2016), but many schools of thought consider complete TGA and DORV to be mutually exclusive.

III. Tricuspid atresia

Tricuspid atresia encompasses a group of CHD where there is an absence of the tricuspid valve. Most atretic lesions are described as muscular, where there is simply a thickening where the normal valve should be. Other forms can include membranous type, Ebstein type, valvular type, and atrioventricular type (Rao, 1980). No distinct cause of tricuspid atresia has been identified, but association with other developmental diseases such as Down syndrome or early-gestational viral illness may be associated with failure of the tricuspid valve leaflets to form

appropriately. It is frequently classified by the associated defects and positioning of the great vessels:

type I: normally related great arteries

type II: d-TGA

type III: malposition of the great arteries but not complete transposition

type IV: common arterial trunk

Typically there is a diminutive right ventricle as well as a PFO to allow venous return to the left heart (Rao, 2019).

Atresia of the tricuspid valve prevents flow of deoxygenated blood through the right heart to the lungs, vastly decreasing pulmonary perfusion. In order for blood to leave the right heart, a shunting lesion must be present to allow the blood to flow into the left heart. Because of this mixing of oxygenated and deoxygenated blood and the low pulmonary flow, the infant becomes cyanotic.

Repair is extensive and largely dependent on the manifestation of other defects with the tricuspid atresia. In most cases, where there is diminished pulmonary blood flow, procedures must be undertaken to increase pulmonary blood flow. This can include ductal stenting, VSD enlargement, resection of right ventricular outflow tract (RVOT) obstruction, balloon pulmonary valvuloplasty, atrial septostomy, and modified BT shunt. Of these procedures, modified BT shunt is the most commonly used. However, for patients with TGA, there may be increased pulmonary blood flow, so pulmonary banding may be pursued. These palliative procedures are considered stage I of a 3-part repair. At about 6 months of age, stage II is pursued, which involves a bidirectional Glenn procedure to direct superior venous blood flow into both branch pulmonary arteries. Additional obstructive or regurgitant lesions are repaired at this stage.

Finally, stage III starts about 1 year after the bidirectional Glenn procedure and consists of completion of the Fontan procedure -- direction of the inferior vena cava into the branch pulmonary arteries. Significant MAPCAs must be occluded at this time. If the fenestration left by the Fontan procedure is significant, it can be closed 6 months to 1 year following the start of stage III (Rao, 2019). Due to the extensive nature of these surgeries, they are staged to allow the pulmonary vascular bed to accommodate the increase in pulmonary blood flow. Additionally, pulmonary vascular resistance decreases after the neonatal period; low resistance in this pathway is critical to success, as the Fontan circulation effectively relies on a single ventricle to power both vascular beds (Sommer et al., 2008a).

In veterinary medicine, tricuspid atresia has been reported in the alpaca, horse, sheep, and dog (Gumbrell, 1970; Meurs, Miller, Hanson, & Honnas, 1997; Slack, Johns, Van Eps, & Reef, 2008; van der Linde-Sipman & van den Ingh, 1979). Findings have been confirmed on post-mortem with no therapies detailed.

IV. Tetralogy of Fallot

Tetralogy of Fallot (TOF) is arguably the most well-known of the cyanotic congenital heart defects, with a long history of descriptions dating back to Niels Stensen in 1671. It was not until Etienne-Louis Arthur Fallot described the disease in 1888 as *la maladie bleu* that it was recognized as a single disease entity; the complex later received the name tetralogy of Fallot from the cardiologist Maude Abbott in 1924 (Van Praagh, 2009). TOF consists of 4 components: pulmonary stenosis, overriding or dextropositioned aorta, ventricular septal defect, and right ventricular hypertrophy. Occasionally, presence of an atrial septal defect (ASD) or PFO will lead to use of the term pentalogy of Fallot. Pulmonary stenosis can be subvalvar, valvar, or

supravalvar and may extend to the pulmonary branches; it may also manifest as multiple levels of stenosis or, most severely, pulmonary atresia. Most cases have a perimembranous VSD, but other VSDs can also be present. TOF is believed to arise from a single developmental defect at the distal bulbus cordis and proximal truncus arteriosus that leads to failure to form the proximal outflow tracts.

The VSD in TOF is generally large and unrestricted, allowing admixture of oxygenated and deoxygenated blood. This in combination with the pulmonary stenosis, allows deoxygenated blood to be more easily delivered through the overriding aorta to the systemic circulation. If a large amount of deoxygenated blood is delivered, then the patient will become cyanotic; however, not all patients are initially profoundly cyanotic. Eisenmenger physiology develops, further encouraging deoxygenated blood to the aorta through a right to left shunting VSD, and progressive cyanosis ensues.

Depending on the extent of right to left shunt, patients may not be clinically affected immediately and may be several months of age before clinical signs are noted. Surgical repair for classic TOF aims to correct the anatomic defects by VSD patching to direct left ventricular flow into the aorta and relief of the pulmonary obstruction with or without a transannular patch (Rao, 2019). The Castañeda doctrine has promoted definitive repair as soon as the patient needs it, avoiding palliative surgeries such as modified BT shunt if possible (Van Praagh, 2009). Other palliative procedures to allow further patient growth include ductal stenting, pulmonary balloon valvuloplasty, and RVOT stenting. Notably in premature babies, these palliative procedures may be needed until definitive surgery can be performed later. In cases of TOF with pulmonary atresia, these patients are ductal dependent, and if definitive surgery cannot immediately be performed, then a procedure to increase pulmonary blood flow is needed. Most commonly, this

is done via a modified BT shunt. It is often difficult to perform ductal stenting in these patients because the PDA is long and tortuous. In other cases of pulmonary atresia, the patient is not ductal dependent but has MAPCAs. These patients are often able to maintain appropriate oxygen saturation, but if not, opening the ductus or an aortopulmonary shunt such as a modified BT shunt is needed. For these patients, surgery cannot be pursued until later when the vessels are large enough to anastomose and construct into branch pulmonary arteries.

TOF has comparatively more documentation in veterinary medicine than the other cyanotic heart defects. It has been documented to occur in the dog, cat, sheep, cattle, domestic ferret, Bengal tiger, European brown bear, and European beaver (Ågren, Söderberg, & Mörner, 2005; Chetboul et al., 2016; Lacasta et al., 2011; Mohamed et al., 2004; Pazzi, Lim, & Steyl, 2014; Wenger et al., 2010). A number of retrospective cases series have been performed. One addressing all CHD in companion animals estimates an incidence of 0.6% of CHD are TOF (Tidholm, 1997). Another study in dogs and cats found that terrier breeds were overrepresented and that patients with no to low-grade heart murmurs at the time of diagnosis fared worse. Median age at cardiac-related death was 23.4 months with no difference between cats and dogs. Both species had individuals that lived for greater than 5 years; however, most individuals did have clinical signs, and some palliative medical management was followed (Chetboul et al., 2016). Surgical palliation and definitive repair have been reported for TOF in dogs. Balloon dilation of the pulmonary stenosis has been reported with good initial success but possible return of signs after 9 months (Oguchi et al., 1999; Weder, Ames, Kellihan, Bright, & Orton, 2016). Brockman et al. performed modified BT shunt in 6 dogs, of which 5 survived the post-operative period. The authors reported improvement of signs and no shunt obstruction. Of the patients that were deceased by the time of publication, the 2 that survived immediately post-operatively died

6 years after the procedure. Definitive surgical repair has also been described in 4 dogs with good outcome (Herrtage, Hall, & English, 1983; Lew, Fowler, McKay, Egger, & Rosin, 1998; Orton, Mama, Hellyer, & Hackett, 2001). In 1 case, the dog continued to die of heart failure 2 years post-procedure, but the other 3 cases were free of clinical signs at the time of respective publications.

V. Total anomalous pulmonary venous connection

Total anomalous pulmonary venous connection (TAPVC) includes a host of anatomic variations that involve oxygenated blood from the lungs returning to the heart in abnormal positions. Embryologically, the common pulmonary vein turns into 4 independent pulmonary veins that join into the left atrial wall with regression of the pulmonary-splanchnic connections. When early atresia or malposition of the common pulmonary vein occurs before all of the connections have regressed, anomalous venous connections are formed (Katre, Burns, Murillo, Lane, & Restrepo, 2012). TAPVC are categorized as supracardiac, cardiac, and infracardiac (or infra-diaphragmatic); if more than one type is present, then they are classified as mixed type. Supracardiac anomalous vessels converge to drain into the superior vena cava, azygos vein, or the brachiocephalic vein. Cardiac anomalous return occurs directly into the coronary sinus or right atrium. Infracardiac drainage refers to anomalous vessels that drain into the inferior vena cava, hepatic vein, portal vein, or persistent ductus venosus; all connections occur below the diaphragm. Partial anomalous pulmonary venous connection, where at least 1 pulmonary vein drains appropriately into the left atrium, can also occur (Ezon et al., 2015). TAPVC can also be physiologically categorized as obstructive or non-obstructive based on the amount of venous

return. Most supra-diaphragmatic (supracardiac and cardiac types) vessels are non-obstructive (Rao, 2019).

Admixture of the oxygenated blood from the lungs into the deoxygenated right heart system, which then flows to the systemic circulation, results in cyanosis. Most patients have an ASD or PFO, but some kind of right to left shunt is necessary for survival to allow the blood to enter systemic circulation.

Patients with supracardiac or infracardiac type of TAPVC generally have anomalous vessels that converge into a common pulmonary vein that then returns blood to the right heart system inappropriately. Atrial septostomies can be performed to improve return to the left heart through the ASD or PFO, but typically correction of the anomalous return is pursued when identified as infants. This involves redirection of that common pulmonary vein into the left atrium. For patients with cardiac type of TAVPC that has drainage into the coronary sinus, the common wall between the coronary sinus and left atrium is removed, and the sinus is separated from the right atrium, allowing oxygenated blood to flow unmixed into the left heart. Patients with mixed type of TAPVC tend to not have a large common pulmonary vein that can be redirected. Thus, these patients may benefit from atrial septostomy until the anomalous vessels are large enough to be individually redirected to the left atrium (Rao, 2019). As long as the disease is not obstructive, the patient can be palliated with maintenance of a right to left shunt.

TAPVC has been reported in the veterinary literature very rarely. There are reported cases in the foal, puppy, and in a domestic chick (Aihara et al., 2013; Bode et al., 2019; Diaz, Desrochers, Hoffmann, & Reef, 2005). All cases presented with an ASD or PFO. Partial anomalous pulmonary venous connection has been more commonly reported in the veterinary population but is still rare (Hsueh, Yang, Lin, & Chan, 2020; Mizuno et al., 2020; Morita,

Hoshino, Kobayashi, & Endo, 2022; Nicolson, Daley, Makara, & Beijerink, 2015; Thorn, Ford, & Sleeper, 2017). These cases may or may not be symptomatic; screening echocardiogram for non-clinical patients was initiated after incidental cardiomegaly was appreciated on work-up for unrelated problem. ASD may or may not be present.

Palliative Shunt Procedures

Numerous aortopulmonary or systemic-to-pulmonary shunts have been developed and trialed through the years to help relieve different cardiac ailments. The following major arterial systemic-to-pulmonary shunts are described: Blalock-Thomas-Taussig shunt, Mee shunt, Potts-Smith-Gibson shunt, and Waterston-Cooley shunt (Santos, Qureshi, Mery, & Shekerdemian, 2020; Yuan & Jing, 2009). An aorta to right ventricular shunt has been documented (Sakurai, Sakurai, Ohashi, & Nishikawa, 2018).

The Blalock-Thomas-Taussig or Blalock-Taussig (BT) shunt traditionally achieved aortopulmonary shunting by directing a subclavian artery end-to-side into the pulmonary artery. Sacrificing the subclavian artery opposite the side of the aortic arch was performed to prevent kinking of the artery. Originally only including autogenous live tissue, it was hoped that the shunt would grow with the patient; however, scar tissue at the anastomosis often limited growth. In addition, it was a time-consuming surgery with extensive dissection that could lead to phrenic nerve injury and poor limb perfusion. Thus, the modified BT shunt uses a graft to connect the subclavian artery and the pulmonary artery. Subclavian steal is still present but the vessel is not fully sacrificed. Issues of shunt patency and scar tissue remain. It has been reported that second surgery or catheter-based intervention can be used to re-establish patency (Bonnet et al., 2015).

The Mee shunt, or Melbourne or central shunt, anastomoses the main pulmonary artery onto the ascending aorta. This increase in flow is to allow for additional development of the branch pulmonary arteries and future repair. Alternatively, a PTFE graft can be placed between the ascending aorta and the main pulmonary artery, known as the Redo-Ecker shunt (Redo & Ecker, 1963). These shunts can allow for increased perfusion to both lungs, can avoid subclavian steal, and can be performed on infants where size of peripheral vessels would be too small. Nevertheless, this does involve entry into the pericardial space, making future surgery in this area more challenging.

In infants with anatomically normal aortic arches, the Potts-Smith-Gibson or Potts shunt connects the descending aorta to the left pulmonary artery. Similarly, the Waterston-Cooley shunts connect the ascending aorta to the right pulmonary artery. In the Waterston shunt the anastomosis is extrapericardial whereas in the Cooley shunt the anastomosis is intrapericardial. Because of the anastomosis into the right or left pulmonary artery directly from the aorta, preferential blood flow occurs in both of these methods. This can lead to pulmonary hypertension and distortion of the addressed pulmonary artery as well as hypoplasia of the opposite pulmonary artery. Both the Potts shunt and Waterston-Cooley shunts can also be technically challenging to close properly at the time of definite surgery. Thus, they are no longer commonly performed.

Of the surgical systemic to pulmonary shunts, the modified BT shunt is the most commonly used in human and veterinary medicine today. It allows good left to right blood flow, is technically easier than many of the other shunts, and it can be reversed relatively well at the time of future procedure. Good relief can be achieved with interventional procedures such as ductal stenting, but in cases that require a large systemic-to-pulmonary flow or have very

abnormal anatomy, surgical intervention is often still elected. There are also many variations to the aforementioned shunts to allow for anatomical anomalies, physiologic abnormalities, and graft differences.

For some cardiac defects, a venous to pulmonary shunt is preferred. The following major venous systemic to pulmonary shunts are described: Glenn shunt and Sano shunt. The Sano shunt directs blood flow from the right ventricle to the pulmonary arteries (Yuan & Jing, 2009). It is typically used in combination with the Norwood procedure, which is used to treat predominantly patients with hypoplastic left heart syndrome but also other conditions with limited left heart flow; the Norwood procedure consists of atrial septectomy, reconstruction of the aorta, and redirection of the pulmonary blood flow from the heart. The Sano shunt is reported to have greater hemodynamic stability than the modified BT shunt with the Norwood procedure because it allows for better diastolic coronary perfusion (Rao, 2019).

The Glenn shunt is often performed as a second surgery following the Norwood procedure, or BT shunt or pulmonary banding for tricuspid atresia. These two steps are part of a three-part surgical journey that ends with the Fontan procedure to create full Fontan circulation (Rao, 2019). Classic Glenn shunt is composed of an anastomosis of the superior vena cava and the right pulmonary artery with disconnection from the main pulmonary artery and left pulmonary system, but bidirectional Glenn shunt is now favored. The bidirectional Glenn shunt is thus named because the superior vena caval flow is directed into the pulmonary arteries bilaterally from the anastomosis to the right pulmonary artery by closing the connection from the superior vena cava to the right atrium (Yuan & Jing, 2009). This directs the entirety of the superior venous blood flow to the pulmonary circulation, so that the lungs learn to accommodate

a greater volume of blood before completion of the Fontan circuit with the inferior venous blood flow.

Ovine Cardiac Model

Sheep have been well established as a model animal for human cardiac and cardiovascular disease. Over the years, sheep have been used to model for TOF, cardiopulmonary bypass, cardiogenic shock, atrioventricular blocking, and myocardial remodeling (Di Vicenti, Westcott, & Lee, 2014; Duchenne et al., 2019; Farraha et al., 2020; Rienzo et al., 2020; Shofti, Zaretzki, Cohen, Engel, & Bar-El, 2004; Valdeomillos et al., 2019). Heart rate and intracardiac pressures are similar to the human values. Measurements of awake continuous arterial blood pressure and heart rate have been established to reliably estimate cardiac output (Liu, Kramer, Khan, Kinsky, & Salinas, 2015). Additionally, cardiac anatomy is similar. There is similar RVOT and pulmonary branch anatomy (Valdeomillos et al., 2019). Atrioventricular valves are similar between humans and sheep, although fibrous continuity between mitral to aortic valves is not present. The ovine tricuspid valve is composed of 3 leaflets, but the anterosuperior leaflet and the inferior leaflets can be fused, making it appear to only have 2 leaflets (“Atlas of Human Cardiac Anatomy,” 2021). Ovine hearts tend to be left coronary dominant, whereas humans are right coronary dominant, but the interlinking of the coronary venous vasculature is similar (Di Vicenti et al., 2014). Sheep also do not develop a significant coronary collateral network, making them good models for myocardial ischemia. Finally, although porcine hearts are more similar to human hearts, porcine models grow too quickly and too large; sheep are more easily managed and grow at slower rates, making them physiologically more comparable when it comes to cardiac remodeling (Farraha et al., 2020).

However, there are some differences. Ovine intraventricular conduction is faster (Duchenne et al., 2019). They are also more apt to developing intractable ventricular fibrillation with cardiac manipulation, short periods of myocardial ischemia, and possibly hypothermia (Shofti et al., 2004). Thoracic volume is similar to human capacity, but carriage as a quadruped leads to different anatomical positioning as well as surgical approach.

Limited description exists for thoracic vasculature in the sheep, with most texts grouping it with bovine vasculature. This has been attempted to be rectified some with cross-sectional imaging; as with bovine anatomy, there is a central brachiocephalic trunk of which all cranial vessels derive (Sizarov, de Bakker, Klein, & Ohlerth, 2014). However, Sizarov's study focused on the branching of the vasculature for intravascular procedures and does not relate these vessels well to thoracic access. Thus, one of the goals of this study was to better annotate the thoracic vasculature beyond describing to it as ruminant vasculature.

Cardiac Work

There are numerous ways documented to measure work performed by the heart. In this work, we review that of pressure-volume loops or PV loops. Briefly, a PV loop records the pressure and volume relationship over time, representing the full cardiac cycle of a ventricle (Boron & Boulpaep, 2012; Hall, 2016). It is measured by a pressure-volume transducer placed in the ventricle of study. The cycle can be broken down into 4 phases as shown in Figure 1.

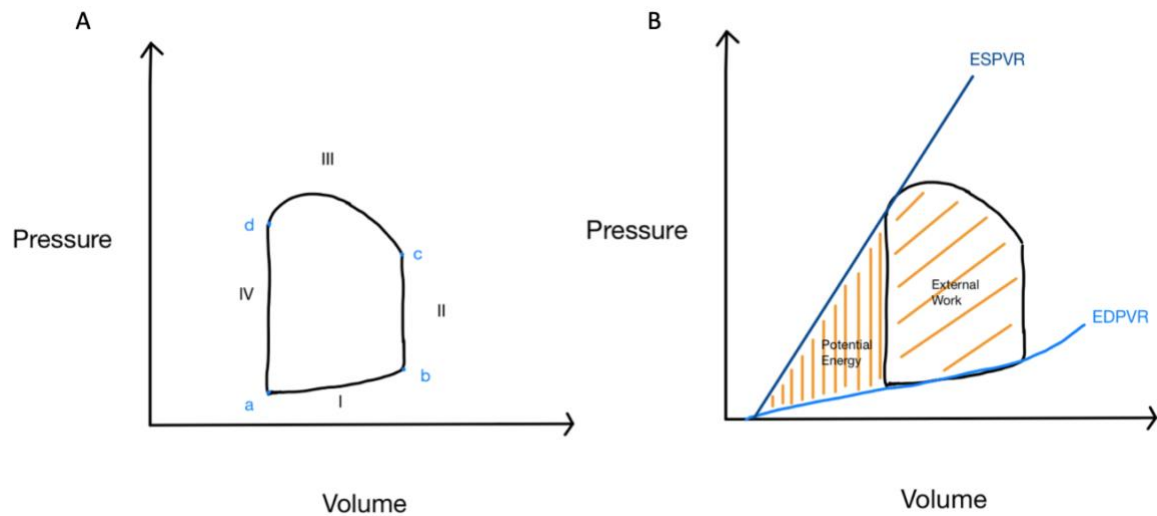


Figure 1: Pressure-volume loop of the left ventricle explained. A. PV loop with physiologic time points.

I. ventricular filling

a. mitral valve opens

II. isovolumetric contraction

b. mitral valve closes

III. ventricular ejection

c. aortic valve opens

IV. isovolumetric relaxation

d. aortic valve closes

B. PV loop has ESPVR and EDPVR curves superimposed. ESPVR is a linear relationship while EDPVR is a curvilinear relationship with the latter part of the curve behaving exponentially.

Together, the curves are able to represent total mechanical work performed by the heart as represented by the pressure volume area (orange). This is composed of the external work performed represented in the PV loop and the potential energy represented in the triangle outside of the PV loop.

Phase I corresponds to ventricular filling during diastole. Phase II corresponds to isovolumetric contraction. Phase III corresponds to ventricular ejection of blood. And, phase IV corresponds to isovolumetric relaxation of the ventricle. It should be noted that the shape represented in Figure 1 is consistent with a PV loop of the left ventricle, but PV loop can be performed for the right ventricle as well. The end of each phase is demarcated by opening or closure of the valves as depicted in Figure 1. End-diastolic volume (EDV) corresponds to the volume at point b. End-systolic volume (ESV) corresponds to the volume at point a. End-systolic pressure (ESP) corresponds to the pressure at point d. Stroke volume, or the volume of blood ejected by the ventricle, can be ascertained by $EDV - ESV$.

Cardiac work can be calculated from PV loop by the area under the curve. External work performed by the heart to eject the blood into circulation is captured by the area within the PV loop. However, additional work is performed as the elastic potential energy, sometimes called internal work, stored to perform the mechanical work; this is captured by the area outside of the PV loop between the end-systolic pressure volume relationship (ESPVR) and end-diastolic pressure volume relationship (EDPVR) curves as shown in Figure 1. These curves are calculated using occlusion maneuvers to reduce preload, changing the volume and monitoring the subsequent cardiac cycle. ESPVR is a linear relationship while EDPVR is a curvilinear relationship with the latter portion of the curve behaving exponentially. The slope of ESPVR represents myocardial contractility and how the maximum pressure is able to respond to changes in volume. The slope of EDPVR is inversely proportional to the compliance of the heart and how the heart is able to fill. Thus, total mechanical work is composed of both the external work and elastic potential energy. It corresponds to the total area in the PV loop combined with the area outside of the loop limited by the pressure-volume relationship curves, and it is aptly named the pressure-volume area (PVA) (Sagawa, Maughan, Suga, & Sunagawa, 1988). It is the total area in orange in Figure 1. Not only does PVA represent the total mechanical work performed by the heart, but it also is a baseline for myocardial oxygen consumption. PV loop transducer can also calculate arterial elastance (E_A), which is a measure of arterial load and ventriculoarterial coupling, as well as Tau, which is a measure of isovolumic relaxation.

Chapter III

Anatomical Study

Methods

Six ovine thoraxes from animals sacrificed from other procedures were offered to the study for examination. For each sheep, the thorax was positioned into right lateral recumbency. Using necropsy blade and shears, the left ribs were transected just below the costochondral junction and as close to the transverse processes as possible. The left-side rib cage was reflected back and the thoracic vasculature documented. The pericardium was excised. Photographs were taken.

Then the heart was harvested including the cranial and caudal vena cava as well as part of the azygos vein, the main pulmonary artery to initial pulmonary branches, the ascending and descending aorta, and the brachiocephalic trunk as cranial as possible. Three of the specimens were dissected to evaluate the cardiac anatomy. The other three specimens were saved for cadaveric proof of concept.

Institutional CTA and magnetic resonance imaging (MRI) of sheep thorax were searched, yielding 3 studies. These were examined to assess cardiac and thoracic vascular anatomy as compared to the cadaveric dissection.

Results

Six thawed thoraxes of adult sheep were examined, and three hearts were fully dissected. The ovine heart is a mammalian heart and is composed of 4 cardiac chambers: right atrium, right ventricle, left atrium and left ventricle. A left aortic arch arises from the left ventricle and gives

rise to an ascending and descending portion of the aorta (Figure 2). No major cranial vasculature from the ascending aorta is present except for a single brachiocephalic trunk, which continues as a single vessel almost to the thoracic inlet. The descending aorta gives rise to the vertebral arteries as it traverses caudally. The pulmonary trunk branches into the left and right pulmonary arteries. Further branching occurred quickly after division into right and left branches. Typically, a very prominent ligamentum arteriosum is present connecting the descending aorta and the pulmonary trunk on the left side; although very robust, dissection of the remnant in these cases never revealed a patent ductus arteriosus. The venous vasculature cranially converges more caudally than branching of the brachiocephalic trunk with vertebral venous supply segmentally converging through the cranial thorax. All cranial vessels return to the cranial vena cava. Caudally, venous return arises from the caudal vena cava, which crosses into the thoracic cavity through the caval foramen and a left azygos vein. The left azygos vein drains prominent branches of the caudal thoracic vertebral venous return, which all converge, crossing just cranial to the hilus of the left cranial lung lobe and enters the right atrium.

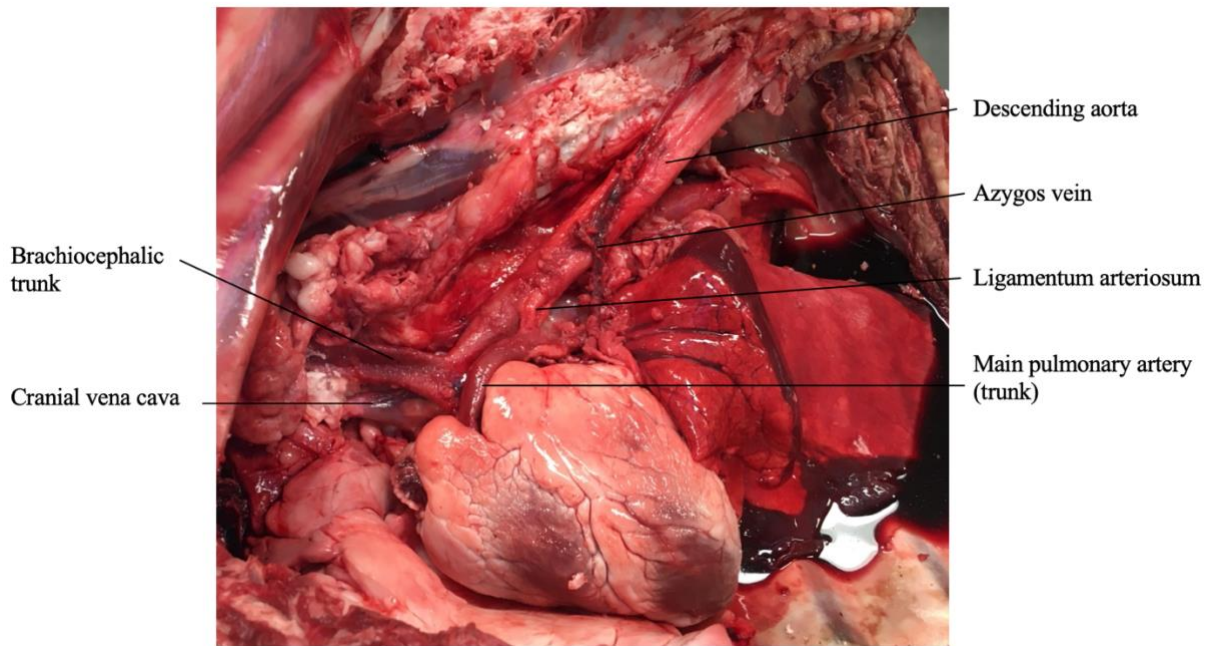


Figure 2: Pictured is thoracic dissection of a deceased adult sheep. The left thoracic rib cage has been reflected cranially and the left lung lobes reflected caudally to expose the vascular anatomy. The pericardium has been resected for better anatomical detail.

Three ovine hearts were dissected. The aortic valve is composed of 3 valve leaflets. The pulmonary valve is composed of 3 valve leaflets. The left atrioventricular valve, or mitral valve, is composed of 2 valve leaflets. And the right atrioventricular valve, or tricuspid valve, is composed of 3 valve leaflets. In 1 heart, the tricuspid valve appeared to have 2 leaflets but likely were fused as previously documented to be present in sheep tricuspid valve anatomy.

The coronary circulation appeared to be left dominant in all cases studied. This was difficult to assess completely in thawed models. As CT images were not cardiac-gated, coronary circulation could not be definitively visualized but were suggestive of left coronary dominance.

Assessment of images supported the bovine arch and branching cranially. Most complete images were appreciated in the CTA, where branching of the left subclavian arises from the brachiocephalic trunk first. This occurs just caudal to the first rib (Figure 3).

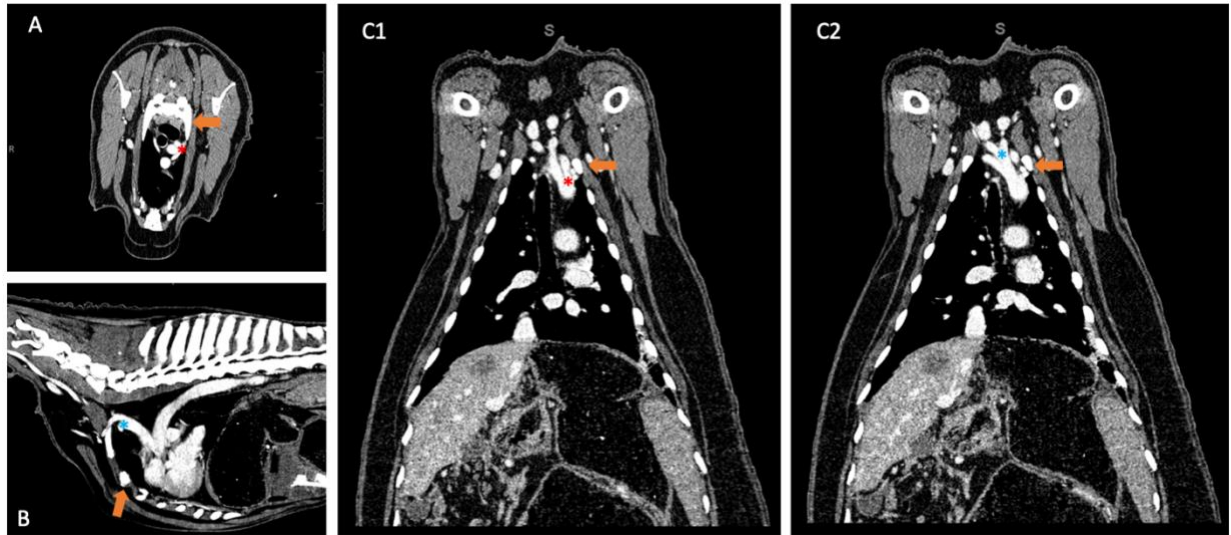


Figure 3: Institutionally available CTA in the venous phase shows branching of the brachiocephalic trunk. A. Transverse section. B. Sagittal rendering. C1 + 2. Dorsal rendering in different planes. Left subclavian arises first as shown by the red asterisk. This is appreciated to be at the level of the rib head of the first rib, just caudal to the body of the first rib (orange arrow). The right subclavian and the carotid arteries arise more cranially in close succession as shown by the blue asterisk, just outside of the thoracic inlet.

Additional branching of the right subclavian and then bilateral carotid arteries then occurs outside of the thorax, just past the thoracic inlet.

Chapter IV

Cadaveric Proof of Concept

Methods

Using the remaining three hearts previously harvested from the ovine thoraxes, evaluation of placement of PTFE shunt was performed. Due to the extensive length of the ovine brachiocephalic trunk before additional branching, modified BT shunt was placed between the brachiocephalic trunk and pulmonary artery. Subclavian artery was not deemed possible due to excessive shunt length and difficulty of surgical dissection.

Approaching the free heart from the left side, the brachiocephalic trunk was isolated with a Satinsky vascular clamp. A stab incision was made with a #11 blade, and then a 4 mm punch was introduced to make the defect. A slanted end of the tubular PTFE graft was sutured in an end-to-side anastomosis over the defect using 5-0 polypropylene with two lines of suture in a simple continuous pattern. The same procedure was then performed at the pulmonary artery using the other end of the PTFE graft.

To ensure that this was reproducible in the ovine thorax, an additional 2 sheep thoraxes were obtained from animals sacrificed from other procedures. For each sheep, the thorax was placed in right lateral recumbency. An intercostal thoracotomy at the left third intercostal space was performed, incising through the cutaneous trunci, latissimus dorsi, scalenus, serratus ventralis, and pectoralis muscles. Finochetto retractors were introduced to improve visualization. Then, after removing connective and adipose tissues, the brachiocephalic trunk was isolated with a Satinsky vascular clamp. A stab incision was made with a #11 blade, and then a 5 mm punch introduced to make the defect. A slanted end of the 6 mm tubular PTFE graft was sutured in an

end-to-side anastomosis over the defect using 5-0 polypropylene with two lines of suture in a simple continuous pattern. In order to visualize the pulmonary artery, the pericardium was incised. The same procedure was then performed at the pulmonary artery using the other end of the PTFE graft.

Results

Three hearts were used to perfect surgical technique before attempting surgical procedure in 2 thawed sheep thoraxes. As previously mentioned, the thoracic vascular anatomy was not conducive to placement of a modified BT shunt from a subclavian artery to the pulmonary artery due to the cranial nature of the subclavian arteries. However, placement of the graft from the brachiocephalic trunk to the main pulmonary artery allowed a pathway without kinking and relatively short length. Thus, cadaveric practice yielded a modified shunt from a left approach from the brachiocephalic trunk to the main pulmonary artery (Figure 4).

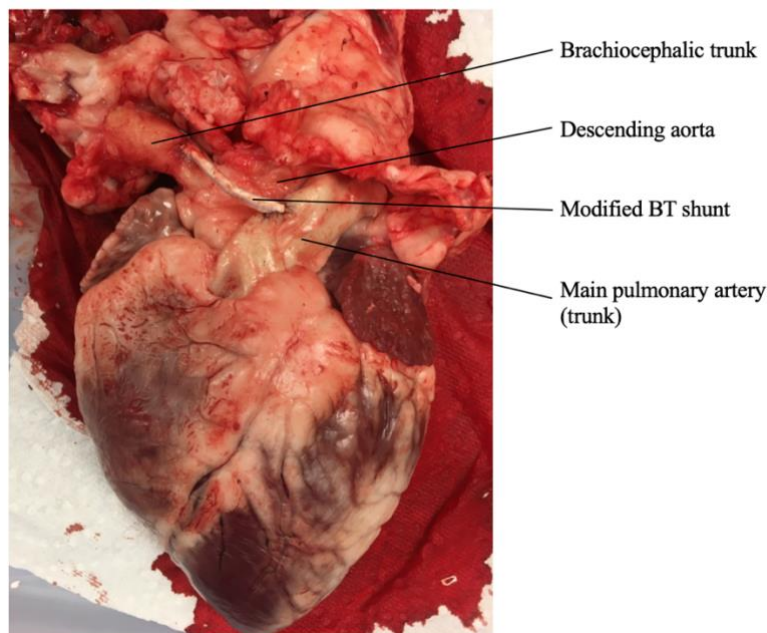


Figure 4: Cadaveric model of the modified BT shunt to be performed from a left intercostal approach.

Thoracic attempts indicated the extremely difficult nature of exposure. Thawed samples have limited thoracic compliance, which resulted in rib fracture with use of the Finochetto retractors in 1 out of the 2 cases. Attempts to find a left subclavian artery were futile through a left intercostal thoracotomy in these models, cementing use of the brachiocephalic trunk.

Chapter V

Pilot Live Sheep Study

Methods

Six female, young adult, Rambouillet sheep were entered into the study under institutional IUCAC protocol # 2301 Development of ovine model to evaluate Blalock-Taussig shunts.

I. Anesthesia

Sheep were anesthetized according to institution IUCAC and preclinical surgical research laboratory protocol. Briefly, they were premedicated with buprenorphine and ketamine, induced with propofol, and then intubated and maintained on inhalant anesthesia. Monitoring for invasive arterial blood pressure, temperature, pulse oximetry, and electrocardiogram were initiated and maintained throughout procedures.

II. Surgery

The patient was placed in right lateral recumbency. The left thorax, left cervical area, and left inguinal area were clipped, cleaned, and prepped for surgery. The patient was draped in standard aseptic fashion. The left jugular vein was then accessed with an 18g IVC. Using a modified Seldinger technique, an 8 Fr catheter was introduced along an introducer; this was secured with 2-0 nylon in a simple interrupted suture. A Swan-Ganz catheter was then introduced in the lumen of the jugular catheter. Pulmonary artery pressures were then measured and recorded.

The left femoral artery was palpated. When possible, an 18 g IVC was introduced, and, using a modified Seldinger technique, a 6 Fr catheter was introduced. If this was not possible, a femoral cut down was performed. This catheter was then secured with 2-0 nylon in a simple interrupted suture. A PV loop transducer was then introduced in the lumen of the femoral catheter and placed with fluoroscopic guidance into the left ventricle. The machine was calibrated and then LV readings performed. When possible, occlusion of the caudal vena cava was performed and occlusion readings performed. When possible, the PV loop transducer was then introduced in the lumen of the jugular catheter, and RV readings were performed with and without occlusion.

A standard intercostal approach to the left 3rd intercostal space was made with electrocautery, incising through the cutaneous trunci, latissimus dorsi, scalenus, serratus ventralis, and pectoralis muscles. In one sheep to improve visualization, the left 3rd rib was resected. Hemostasis was achieved with electrocautery. The chest was entered, and the lungs were packed off dorsally with laparotomy sponges; Finochetto retractors were introduced to improve visualization. A modified BT shunt was placed using a 6mm tubular PTFE graft or treated 8mm tubular PTFE graft connecting the brachiocephalic trunk to the pulmonary artery. First, the brachiocephalic trunk was isolated, and then partially occluded with a Satinsky vascular clamp. A stab incision was made with a #11 blade, and then a 5 mm punch introduced to make the defect. A slanted end of the PTFE graft sutured in an end-to-side anastomosis over the defect using 5-0 polypropylene using two lines of suture in a simple continuous pattern. If a suture gap was noted, a single simple interrupted suture placed. The same procedure was then performed at the pulmonary artery using the other end of the PTFE graft; if visualization was

difficult, the pericardium was excised. Pulmonary artery pressures were then measured and recorded. PV loop was performed when possible.

The chest was lavaged with 1L of sterile saline and suctioned. A 20 Fr chest tube was placed with a trocar and fastened with 2-0 nylon in a Chinese fingertrap. The chest wall was closed with 1 Maxon around the adjacent ribs in a simple interrupted pattern. The musculature was closed with 3-0 Biosyn in a simple continuous pattern. The SQ layer was closed with 3-0 Biosyn in a running simple continuous pattern. The skin was closed with 2-0 nylon in a simple continuous pattern.

III. Post-operative Care

The sheep were recovered from anesthesia under the care of the livestock hospital or laboratory animal veterinary staff pending availability. All were treated with PPG 3 million units SQ q24h, phenylbutazone 1g PO q24h, and fentanyl patch 150mcg total transdermal for 5 days post-operatively. Buprenorphine 0.1 mg/kg SQ was administered peri-operatively, and rescue doses were offered if needed. Heparin 50 mcg/kg IV or SQ was administered every 8 hours for the first 3 days. Physical exams were performed twice a day for the first week post-operatively. Standard husbandry was performed. When companion sheep was lost, an additional was pulled from another study if possible to provide companionship.

Acute-term sheep were maintained for 2 weeks post-operatively. Long-term sheep were maintained for 3 months post-operatively. After initial surgical medications were completed, sheep were allowed to recover relatively undisturbed. Biweekly physical exams were performed to assess for general health and heart murmurs.

IV. Sacrifice

At appropriate term, sheep were returned to the surgical suite for cardiac measurements. They were induced under anesthesia and placed in right lateral recumbency.

The left jugular vein was then accessed with an 18g IVC. Using a modified Seldinger technique, two 8 Fr catheter were introduced along an introducer; these were secured with 2-0 nylon in a simple interrupted suture. A Swan-Ganz catheter was then introduced in the lumen of the jugular catheter. Pulmonary artery pressures were then measured and recorded.

The left femoral artery was palpated. When possible, an 18 g IVC was introduced, and, using a modified Seldinger technique, a 6 Fr catheter was introduced. If this was not possible, a femoral cut down was performed. This catheter was then secured with 2-0 nylon in a simple interrupted suture. As the femoral artery had been ligated in sheep #6, left carotid artery access was acquired instead, and a 6 Fr catheter introduced and secured. A PV loop transducer was then introduced in the lumen of the arterial catheter and placed with fluoroscopic guidance into the left ventricle. The machine was calibrated and then LV readings performed. When possible, occlusion of the caudal vena cava was performed and occlusion readings performed. When possible, the PV loop transducer was then introduced in the lumen of the jugular catheter, and RV readings were performed with and without occlusion.

When all readings were performed, the sheep was euthanized with pentobarbital. Cardiopulmonary arrest was confirmed.

A gross necropsy was performed noting any thoracic abnormalities. The heart was grossly assessed. The shunt was harvested and assessed for adhesion and thrombosis formation.

Results

I. Surgical Outcome

Six young adult, female, Rambouillet sheep were enrolled in the study. Two were enrolled in a short-term study of 2 weeks, and the other 4 were enrolled in a long-term study of 3 months. All sheep were overtly healthy when selected to be enrolled by laboratory animal staff. Enrollment and outcomes are noted in table 1.

Table 1: Summary of enrollment and outcomes of sheep in modified BT shunt study.

Sheep	Length of study	Graft	Outcome
1	Acute	PTFE	Survived, partial occlusion
2	Acute	PTFE	Survived, partial occlusion
3	Chronic	PTFE	Deceased, intra-operative hemorrhage
4	Chronic	PTFE	Survived, full occlusion. Frequent premature ventricular complexes present prior to study intervention. Survived surgery, found deceased following day. Suspect death secondary to blood loss from catherization.
5	Chronic	Treated	Survived, partial occlusion
6	Chronic	Treated	Survived, partial occlusion

Implant placement was possible in 5 out of 6 sheep (Figure 5). In the third sheep of the study, the brachiocephalic trunk was difficult to find due to the severe overconditioning of the animal. This led to hemorrhage from a tear in the friable brachiocephalic trunk as well as small vasculature in the adipose tissue. Due to the friable nature of the trunk, repair was not possible, and the sheep was humanely euthanized under anesthesia. Sheep #3 was not recovered due to irreparable intraoperative hemorrhage.

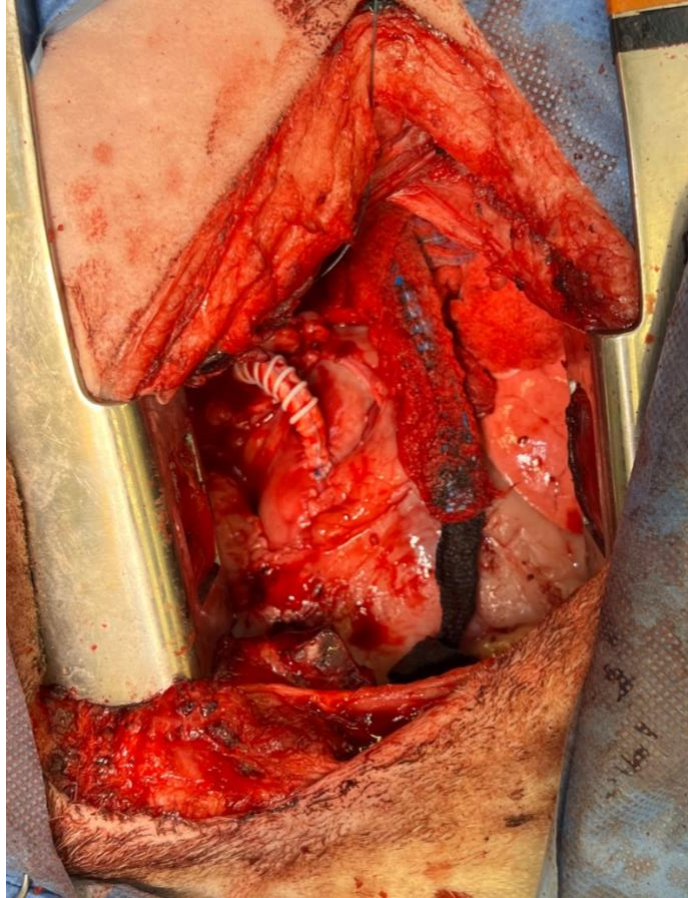


Figure 5: Intraoperative photo of successful placement of non-treated 6mm tubular PTFE shunt from the brachiocephalic trunk to the pulmonary artery.

Other complications occurred. It was noted that in sheep #4, premature ventricular complexes were noted shortly after initiation of anesthesia, prior to any catheterization or surgical intervention. Data collection was severely impeded at time of initial surgery and at sacrifice by the arrhythmia. Arrhythmia were noted in all thoracic auscultation performed throughout the survival period. Sheep #5 was noted to have substantial hemorrhage after removal of femoral artery catheter. Intravenous crystalloid fluid therapy was initiated after surgery for several hours. The patient remained stable overnight with no obvious additional bleeding. Unfortunately, she was found deceased in the morning possibly from delayed hemorrhage at the jugular catheter site, or continued bleeding or sequela from initial hemorrhage at the femoral site. No thoracic hemorrhage was noted.

Post-operatively, no murmurs were noted except for in sheep #6. Continued arrhythmia was noted in sheep #4 through the remainder of the study, but she did not appear to be overly affected. No sheep had any overt clinical sign from the procedure.

II. Cardiac Remodeling

Swan-Ganz catheterization and PV loop transduction in the left ventricle was performed in all sheep at some point in the study. Right ventricular PV loop measurements were performed in sheep #1 and #6 at sacrifice. Results for left heart measurements are available in Table 2.

Table 2: Summary of left heart cardiac data. Blanks in data are from lack of measurement on that timepoint.

Sheep	Baseline										
	HR (bpm)	CO (L/min)	ESP (mmHg)	EDP (mmHg)	EDV (mL)	SV (mL)	SW (mmHg*mL)	dP/dt max (mmHg/s)	Ea (mmHg/mL)	Tau (ms)	PVA (mmHg*mL)
1	90	6.1									
2	70	4.7	89.17	12.16	220.3	58.51	4828	1664	1.524	51.9	
3	86	6.6	91.4	19.64	104.8	47.25	3689	1711	1.935	70.12	
4	78	5.0	93.07	25.41	525	37	4205	957.1	1.549	85.96	
5	99	5.2	104.1	23.53	104.1	41.3	4124	1195	2.543	69.91	
6	70	4.7	97.93	27.82	112	36.46	2816	933.6	2.687	102.5	
Average	82.167	5.38	95.134	21.712	213.24	44.104	3932.4	1292.14	2.0476	76.08	
Initial surgery, post-shunt placement											
1											
2	95	7.9	86.23	13.42	231	56.8	4457	1655	1.524	54.52	
3											
4	94	5.8									
5	118	8.8	99.88	16.85	244.7	100.7	8956	2841	0.9928	42.59	
6	85	7.8	111.1	19.28	135.6	62.85	6144	1822	1.768	60.2	
Average	98	7.58	99.07	16.52	203.77	73.45	6519.00	2106.00	1.43	52.44	
Sacrifice											
1	92	8.2	104.1	9.336	623.6	85.81	8503	1946	1.2	42.6	20080
2	124	10.7	129	14.98	607.1	42.18	5091	1817	3.065	34.11	20018
3											
4	100	5.1	94.46	13.52	101.5	26.46	2202	1237	3.642	70.1	18599
5											
6	116	3.8	104.8	17.78	144.6	32.28	2618	1789	3.249	53.92	4879.8
Average (acute)	108	9.45	116.55	12.158	615.35	63.995	6797	1881.5	2.1325	38.36	20049
Average (chronic)	108	4.45	99.63	15.65	123.05	29.37	2410	1513	3.4455	62.01	11739.4

As sheep #1 was the first patient, troubleshooting of the procedure precluded measurements at the initial surgery. Sheep #3 was only alive for baseline measurements. Sheep #5 was no longer alive for measurements at sacrifice. Due to the persistent arrhythmia following BT shunt placement in sheep #4, measurements could not be performed immediately post-placement. Nevertheless, baseline curves could be generated from runs of good tracings or taking long periods of tracing and removing aberrant results for the arrhythmic sheep (Figure 6).

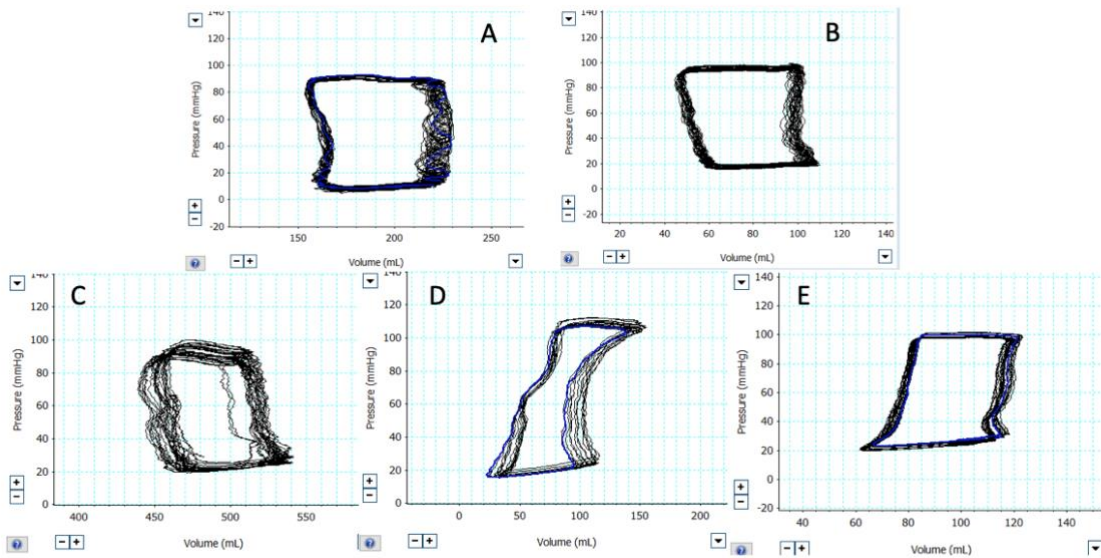


Figure 6: Baseline PV loops of sheep prior to placement of BT shunt. A. Sheep 2. B. Sheep 3. C. Sheep 4. Multiple data points were removed that corresponded to arrhythmogenic heart beats. D. Sheep 5. E. Sheep 6.

Due to the high mortality rate prior to final study (33% of total, 50% of chronic sheep), it was not possible to statistically analyze the data. However, across sheep, heart rate increased following BT shunt placement and continued to increase with cardiac remodeling at the time of sacrifice. Cardiac output noticeably increased immediately post shunt placement and at the 2-week sacrifice; however, it decreased in the chronic study subjects after shunt placement to 3-month sacrifice. E_A increased in both study groups. ESP and EDP were similar throughout the study. Conclusions that rely on accurate volume measurement were hard to make, as the arrhythmia of sheep #4 did not allow for good saline calibration despite numerous attempts. Ultimately, saline calibration had to be foregone, which affected volume data in the final results. Thus, changes in volume are best viewed relatively, but even comparisons of averages are difficult. Given the paucity of data for right heart measurements and no baseline data, no conclusions can be drawn.

PVA was derived from occlusion data and generated ESPVR and EDPVR curves using a similar manner (Figures 7).

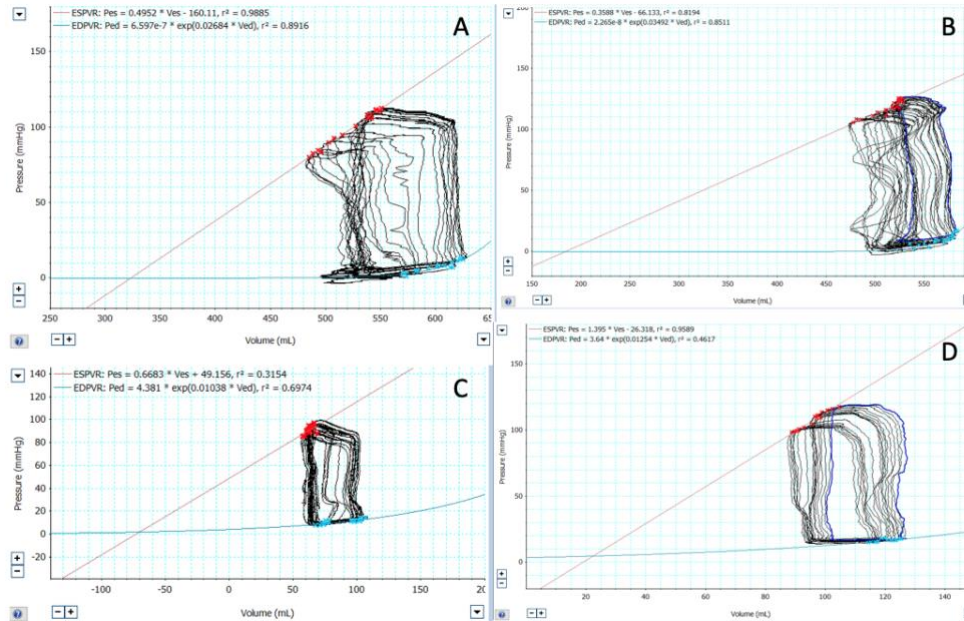


Figure 7: Occlusion graphs obtained at sacrifice. A. Sheep 1. B. Sheep 2. C. Sheep 4. D. Sheep 6.

Curves generated appeared to be well generated except for sheep #4, where arrhythmia prevented appropriate saline calibration. Due to the volume being affected by saline calibration, the point where ESPVR = EDPVR is not physiologically possible. It was difficult to make conclusions from this data, as occlusion at initial surgery was not able to be successfully performed.

III. Necropsy and Shunt Patency

In the acute phase, sheep #1 and #2 were sacrificed at 2 weeks. Murmurs were not appreciated prior to anesthesia and sacrifice. Gross necropsy did not show obvious signs of congestive heart failure. Mild adhesions were present on the external surface of the PTFE graft, but no adhesions to the thoracic wall had been formed. Dissection of the graft showed initial

thrombosis formation in both grafts (Figure 8). Despite material in both grafts, they remained patent during this time point.

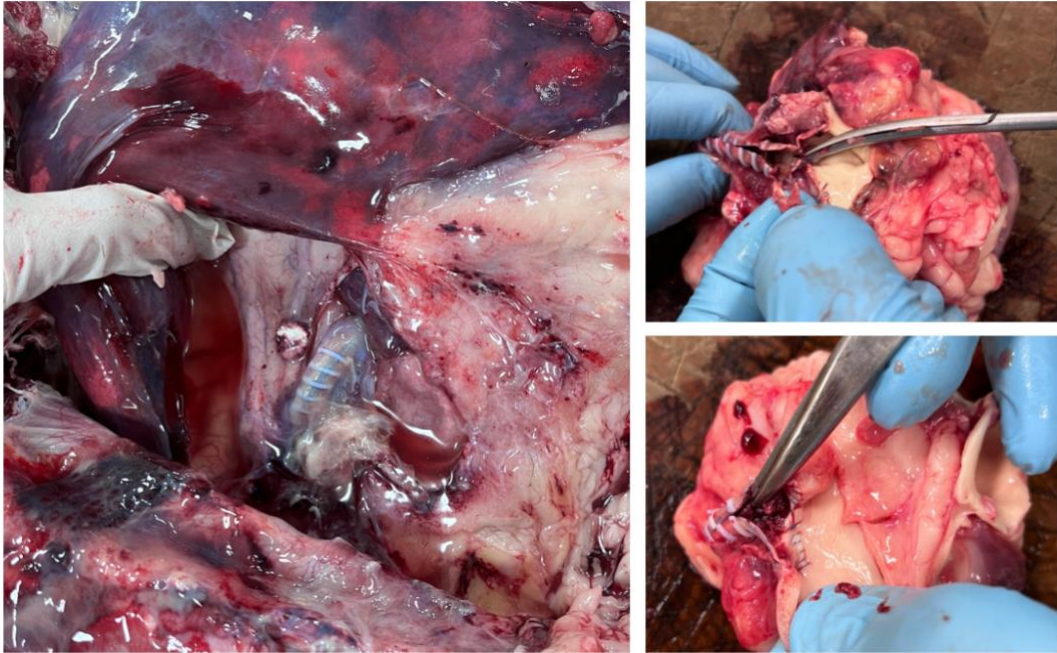


Figure 8: Adhesions in the thoracic cavity are evident around the PTFE shunt at the time of necropsy 2 weeks after surgical procedure (left). In both sheep, thrombotic material was present in the PTFE shunts, but the shunts were only partially occluded (right).

For the 2 sheep that survived the chronic study, no murmur was noted for sheep #4, though arrhythmia was present, and a grade 3/6 left basilar systolic murmur was noted in sheep #6. Gross necropsy did not show obvious signs of congestive heart failure, though it was noted that sheep #6 did have multiple tapeworm hydatid cysts present. Extensive adhesions had formed in the thoracic cavity of both patients (Figure 9).

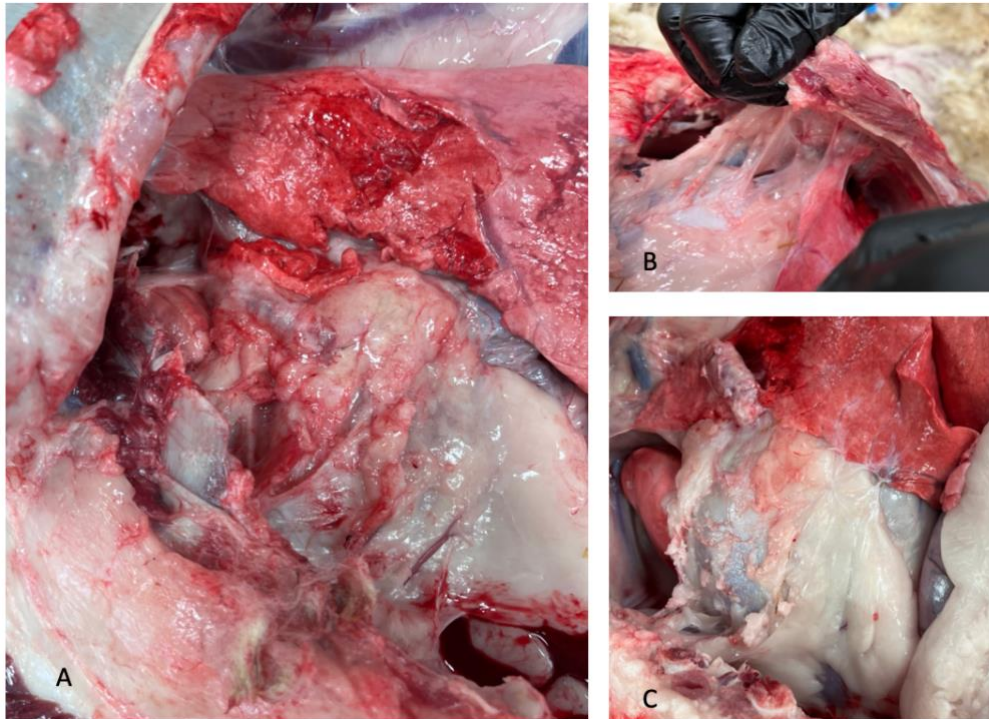


Figure 9: Post-mortem photographs of sheep enrolled in chronic study. A. Sheep #4 in right lateral recumbency (cranial is left) with adhesions obscuring the cardiac silhouette and effacing the left lung lobes. B. Sheep #6 with profound adhesions to the thoracic wall requiring resection with a blade to approach the surgical site. C. Shunt in sheep #6 with minimal adhesions to the actual graft but extensive adhesions surrounding the surgical site. Defect is visible where adhesions were resected for better exposure. Left cranial lung lobe has become entrapped medial to the graft and was adhered.

Shunt was not patent in sheep #4 and occluded throughout much of the shunt as well as fully at both ends. Thrombotic material was present throughout the shunt, with both ends being fully sealed. The material was relatively adhered to the shunt and difficult to remove as was the case with the PTFE shunts from sheep #1 and 2.

The treated shunt of sheep #5 was patent, which was expected given the short survival period (1 day) following surgery. A blood clot was present within as a post-mortem change, but no adhesion to the shunt was present. The treated shunt was partially patent in sheep #6 (Figure 10). Occlusion was predominantly at the aorta anastomosis with the thrombus extending from the suture site; the pulmonary end was fully patent. A probe was still admissible into the shunt at the

thrombus unlike in sheep #4, where no probing was possible. Notably, the material was easy to retract from the wall of the treated shunt in sheep #6 unlike with the PTFE shunts.

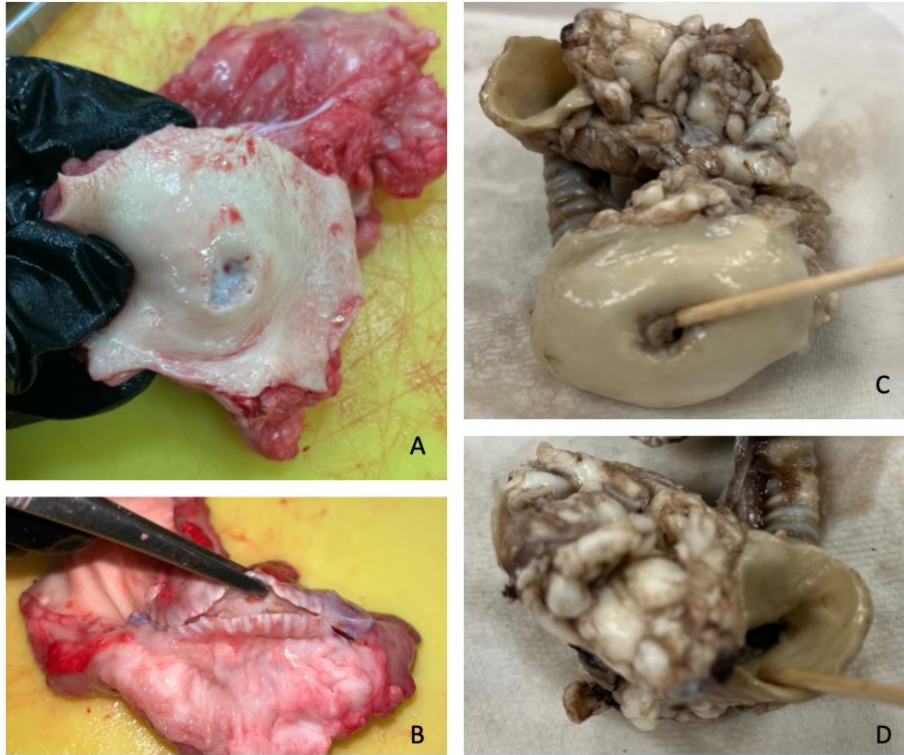


Figure 10: Post-mortem evaluation of shunts patency. A. Sheep #4 PTFE shunt was fully occluded at both entrances at the time of sacrifice. B. PTFE shunt was partially occluded in the body of the shunt with thrombus being notably adhered to the shunt wall. C. Sheep #6 had shunt entrance at the aortic anastomosis significantly partially occluded, but probe was able to enter at the noted point on one side. D. Pulmonary anastomosis was not occluded with no thrombotic material present.

Chapter VI

Discussion, Conclusions and Recommendations

Discussion

This pilot study aimed to better describe ovine thoracic vasculature anatomy, to develop a model for placement of a modified BT shunt in sheep, and to evaluate whether hyaluronan-treated shunts would have decreased thrombosis and adherence.

Firstly, this study was able to better document the thoracic vascular anatomy by thoracic dissection and evaluating institutional CTA and MRI studies. The ovine vascular anatomy does follow a "bovine arch" as previously described in anatomy textbooks and by Sizarov et al. Although their previous imaging study gave better understanding to the branching of the vessels, it was difficult from a surgical anatomy standpoint to understand where to approach. Our study gives the veterinary surgeon a better understanding that branching cranially from the arterial vasculature does not occur until the thoracic inlet. As previously documented, there are 13 ribs, 8 of which have sternal connections (Di Vicenti et al., 2014). Approaches to the heart should occur in the 3rd or 4th intercostal spaces. The great vessels are best accessed through a 3rd left thoracotomy. Those needing access to the brachiocephalic trunk should consider access more cranially. Left thoracotomy does give exposure to most vasculature structures, but multiple thoracotomies or rib resection may need to be considered if needing to reach multiple vessels. Median sternotomy has previously been documented to have a high complication rate in the ovine model, but if large exposure is needed, this could be considered (Shofti et al., 2004).

This study was able to troubleshoot many aspects of the modified BT shunt placement in a sheep. Due to the anatomy, modified BT shunt in the sheep is from the brachiocephalic trunk to

the pulmonary artery. Approach is best through the 3rd left intercostal space. Measurement of cardiac energetics is best performed with left jugular vein and left carotid access. Use of the femoral arteries is certainly possible as it was performed many times in this study, but access was tedious and it possibly led to the demise of one sheep from bleeding post-operatively. It is possible that bleeding would be less problematic if patients were not anti-coagulated, but for the purposes of shunt placement, anti-coagulation was necessary.

The anatomic study did not specifically measure vascular size relative to thoracic dimensions or weight; regardless, likely this would have inaccurate in frozen thawed sheep. Despite most of the sheep being of similar weight, length of catheter needed and size of vasculature was highly variable. Occlusion was difficult to obtain in sheep #4 due to the balloon being insufficiently large to occlude the caudal vena cava. Additionally, some sheep had a distance from the femoral artery access to the left ventricle that was simply too long for some of the equipment. Regardless, long working length of the catheters, sheaths and transducers needed for femoral access gave much less control than when carotid access was sought. Use of a more caudal left carotid access point for the second procedure could allow for use of the left carotid in both procedures.

Cardiac energetics were measured in this study, but due to the high mortality rate, statistics cannot be performed. However, these do provide some baseline measurements for future studies. Additionally, it can be seen that some remodeling does seem to have occurred due to the increase in heart rate and cardiac output. It is possible that 2 weeks is insufficient for cardiac remodeling to occur based on the then decrease in cardiac output for the chronic sheep. Additionally, few adhesions had occurred in the thoracic cavity compared to what was present at 3 months. In addition to the high mortality rate, 1 of the sheep in our chronic study seemed to

have some level of underlying cardiac disease from the arrhythmia present through all stages of the study. This made measurements extremely difficult and unfortunately volume results are very hard to interpret.

Finally, this study evaluated a hyaluronan coating on the PTFE shunt. Grossly, the chronically treated shunt was still partially patent, while the classic PTFE material was not. Technically, a "larger" shunt diameter was used with the treated shunt but this was to allow for shrinkage with the treatment; nevertheless, there is a small chance this could have contributed to the shunt not fully occluding. Notably, the thrombotic material in the treated PTFE shunt was also easily removed from the shunt wall whereas it was very adhered in the classic PTFE shunt. Hyaluronan has been previously documented to prevent adhesions in gynecologic and gastrointestinal procedures as gels or impregnated materials (Mais et al., 2012; Vrijland et al., 2002), so it stands to reason that it should be applicable for reducing adhesions to PTFE. However, the true mechanism by which hyaluronan reduces adhesions is not fully known with speculations of separation of membranes, increased fibrinolysis, and anti-inflammatory properties, which may be less applicable to not live tissue (Gupta, Lall, Srivastava, & Sinha, 2019; Sikkink, Zeebregts, & Reijnen, 2007); thus, further studies in a greater number of patients is necessary to evaluate this claim. Long-term, those using the BT-shunt ovine model should consider anti-coagulants past 3 days post-operatively. As this study was interested in assessing thrombosis and adherence, anti-coagulants were not continued; however, for best results with the model, those using performing BT shunts in sheep in the future should consider.

Conclusions

This pilot study better characterized sheep thoracic anatomy. It examined the use of an ovine model for modified BT shunt. Shunt patency, patient health, and cardiac energetics were evaluated acutely and chronically. Our hypotheses of:

1. There would be cardiac remodeling secondary to BT shunt placement in the ovine model.
2. BT shunts treated with hyaluronan would have decreased thrombosis and adherence when compared to normal PTFE shunts.

were subjectively supported by this short study, but results were complicated by the high mortality-rate associated with our subjects.

Recommendations for Further Study

Some of the limitations in this study that could be improved upon for continued research include:

- Additional enrollment of sheep to provide data for patients lost in this pilot study.
- Use of echocardiogram to document flow through the modified BT shunt and to help document pre-surgical to post-surgical changes. This non-invasive diagnostic may have a hard time acquiring good images of the shunt, especially after adhesion formation. However, this is a diagnostic used every day in human and veterinary medicine that could provide further information on cardiac function.
- Use of histopathology may be helpful to more objectively assess extent of tissue change in the surrounding vascular tissue, mediastinum, thorax, pericardium, and lung parenchyma that is affected by the adhesions.

- Access to the left heart was significantly easier with carotid artery access. Further exploration of access cranially that is ligated at the time of surgery so that more proximal (caudal) access can still be performed at the time of sacrifice is recommended.

REFERENCES

- Ågren, E., Söderberg, A., & Mörner, T. (2005). Fallot's tetralogy in a European brown bear (*Ursus arctos*). *Journal of Wildlife Diseases*, *41*(4), 825–828. <https://doi.org/10.7589/0090-3558-41.4.825>
- Aihara, N., Horiuchi, N., Hikichi, A. N., Ochiai, M., Ishikawa, Y., & Oishi, K. (2013). Total Anomalous Pulmonary Venous Connection in a Chicken. *Avian Diseases*, *57*(1), 140–142.
- Atlas of Human Cardiac Anatomy. (2021). Retrieved from Regents of the University of Minnesota website: <http://www.vhlab.umn.edu/atlas/comparative-anatomy-tutorial/valves.shtml>
- Bernier, P. L., Stefanescu, A., Samoukovic, G., & Tchervenkov, C. I. (2010). The challenge of congenital heart disease worldwide: Epidemiologic and demographic facts. *Seminars in Thoracic and Cardiovascular Surgery: Pediatric Cardiac Surgery Annual*, *13*(1), 26–34. <https://doi.org/10.1053/j.pcsu.2010.02.005>
- Bode, E. F., Longo, M., Breheny, C., Del-Pozo, J., Culshaw, G. J., & Martinez-Pereira, Y. (2019). Total anomalous pulmonary venous connection in a mature dog. *Journal of Veterinary Cardiology*, *21*, 10–17. <https://doi.org/10.1016/j.jvc.2018.11.003>
- Bonnet, M., Petit, J., Lambert, V., Brenot, P., Riou, J. Y., Angel, C. Y., ... Baruteau, A. E. (2015). Catheter-Based Interventions for Modified Blalock–Taussig Shunt Obstruction: A 20-Year Experience. *Pediatric Cardiology*, *36*(4), 835–841. <https://doi.org/10.1007/s00246-014-1086-0>
- Boron, W. F., & Boulpaep, E. L. (2012). *Medical Physiology* (2nd ed.). Philadelphia, PA; USA: Saunders.
- Chetboul, V., Pitsch, I., Tissier, R., Gouni, V., Misbach, C., Trehieu-Sechi, E., ... Bomassi, E. (2016). Epidemiological, clinical, and echocardiographic features and survival times of dogs and cats with tetralogy of fallot: 31 cases (2003–2014). *Journal of the American Veterinary Medical Association*, *249*(8), 909–917. <https://doi.org/10.2460/javma.249.8.909>
- Chuzel, T., Bublot, I., Couturier, L., Nicolier, A., Rivier, P., Mai, W., & Cadoré, J. L. (2007). Persistent truncus arteriosus in a cat. *Journal of Veterinary Cardiology*, *9*(1), 43–46. <https://doi.org/10.1016/j.jvc.2005.06.001>
- Collett, R. W., & Edwards, J. E. (1949). Persistent Truncus Arteriosus: A Classification According to Anatomic Types. *Surgical Clinics of North America*, *29*(4), 1245–1270.
- Di Vicenti, L., Westcott, R., & Lee, C. (2014). Sheep (*Ovis aries*) as a model for cardiovascular surgery and management before, during, and after cardiopulmonary bypass. *Journal of the American Association for Laboratory Animal Science*, *53*(5), 439–448.
- Diaz, O. S., Desrochers, A., Hoffmann, V., & Reef, V. B. (2005). Total anomalous pulmonary venous connection in a foal. *Veterinary Radiology and Ultrasound*, *46*(1), 83–85. <https://doi.org/10.1111/j.1740-8261.2005.00017.x>
- Duchenne, J., Claus, P., Pagourelis, E. D., Mada, R. O., Van Puyvelde, J., Vunckx, K., ... Voigt, J. U. (2019). Sheep can be used as animal model of regional myocardial remodeling and controllable work. *Cardiology Journal*, *26*(4), 375–384. <https://doi.org/10.5603/CJ.a2018.0007>
- Ezon, D. S., Goldberg, J. F., & Kyle, W. B. (2015). *Atlas of Congenital Heart Disease Nomenclature* (R. H. Anderson & R. Van Praagh, Eds.). Houston, Texas: Ezon Educational

Services.

- Farraha, M., Lu, J., Trivic, I., Barry, M. A., Chong, J., Kumar, S., & Kizana, E. (2020). Development of a sheep model of atrioventricular block for the application of novel therapies. *PLoS ONE*, *15*(2), 1–17. <https://doi.org/10.1371/journal.pone.0229092>
- Grünberg, W., van Bruggen, L. W. I., Eisenberg, S. W. F., Weerts, E. A. W. S., & Wolfe, A. (2011). Complete transposition of the aorta and pulmonary artery in a Belgian Blue crossbreed calf: a case report. *BMC Veterinary Research*, *7*, 22. <https://doi.org/10.1186/1746-6148-7-22>
- Gumbrell, R. C. (1970). Atresia of the tricuspid valve in a foal. *New Zealand Veterinary Journal*, *18*(11), 253–256. <https://doi.org/10.1080/00480169.1970.33916>
- Gupta, R. C., Lall, R., Srivastava, A., & Sinha, A. (2019). Hyaluronic acid: Molecular mechanisms and therapeutic trajectory. *Frontiers in Veterinary Science*, *6*(JUN), 1–24. <https://doi.org/10.3389/fvets.2019.00192>
- Hall, J. E. (2016). *Textbook of Medical Physiology* (13th ed.). Philadelphia, PA; USA: Elsevier.
- Herrtage, M. E., Hall, L. W., & English, T. A. H. (1983). Surgical correction of the tetralogy of Fallot in a dog. *Journal of Small Animal Practice*, *24*(2), 51–62. <https://doi.org/10.1111/j.1748-5827.1983.tb00416.x>
- Hsueh, T., Yang, C. C., Lin, S. L., & Chan, I. P. (2020). Symptomatic partial anomalous pulmonary venous connection in a kitten. *Journal of Veterinary Internal Medicine*, *34*(6), 2677–2681. <https://doi.org/10.1111/jvim.15934>
- Jacobs, M. L., & Anderson, R. H. (2012). Rationalising the nomenclature of common arterial trunk. *Cardiology in the Young*, *22*(6), 639–646. <https://doi.org/10.1017/S1047951112001606>
- Jesty, S. A., Wilkins, P. A., Palmer, J. E., & Reef, V. B. (2007). Persistent truncus arteriosus in two Standardbred foals. *Equine Veterinary Education*, *19*(6), 307–311. <https://doi.org/10.2746/095777307X213946>
- Katre, R., Burns, S. K., Murillo, H., Lane, M. J., & Restrepo, C. S. (2012). Anomalous Pulmonary Venous Connections. *Seminars in Ultrasound, CT and MRI*, *33*(6), 485–499. <https://doi.org/10.1053/j.sult.2012.07.001>
- Kochi, M., Sugimoto, K., Kawamoto, S., Inoue, M., & Machida, N. (2021). Persistent truncus arteriosus with an anomalous coronary artery in a cat. *Journal of Veterinary Cardiology*, *35*, 8–13. <https://doi.org/10.1016/j.jvc.2021.02.007>
- Koo, S. T., Leblanc, N. L., Scollan, K. F., & Sisson, D. D. (2016). Complete transposition of the great arteries with double outlet right ventricle in a dog. *Journal of Veterinary Cardiology*, *18*(2), 179–186. <https://doi.org/10.1016/j.jvc.2015.12.005>
- Kurosawa, T. A., Gunasekaran, T., Sanders, R., & Carr, E. (2016). Common arterial trunk in a 3-day-old alpaca cria. *Case Reports in Veterinary Medicine*, 2016. <https://doi.org/10.1155/2016/4609126>
- Lacasta, D., Ruíz, S., Ramos, J. J., Ferrer, L. M., Fernández, A., & Gómez, P. (2011). Short communication: Tetralogy of fallot in a threemonth-old lamb: Clinical, ultrasonographic and laboratory findings. *Veterinary Record*, *169*(3). <https://doi.org/10.1136/vr.d2609>
- Lew, L., Fowler, J., McKay, R., Egger, C., & Rosin, M. (1998). Open-heart correction of tetralogy of fallot in an acyanotic dog. *JAVMA*, *213*, 652–657.
- Liu, N. T., Kramer, G. C., Khan, M. N., Kinsky, M. P., & Salinas, J. (2015). Blood pressure and heart rate from the arterial blood pressure waveform can reliably estimate cardiac output in a conscious sheep model of multiple hemorrhages and resuscitation using computer

- machine learning approaches. *Journal of Trauma and Acute Care Surgery*, 79(4), S85–S92. <https://doi.org/10.1097/TA.0000000000000671>
- Mais, V., Cirronis, M. G., Peiretti, M., Ferrucci, G., Cossu, E., & Melis, G. B. (2012). Efficacy of auto-crosslinked hyaluronan gel for adhesion prevention in laparoscopy and hysteroscopy : a systematic review and meta-analysis of randomized controlled trials. *European Journal of Obstetrics and Gynecology*, 160(1), 1–5. <https://doi.org/10.1016/j.ejogrb.2011.08.002>
- Markovic, L. E., Scansen, B. A., & Potter, B. M. (2017). Role of computed tomography angiography in the differentiation of feline truncus arteriosus communis from pulmonary atresia with ventricular septal defect. *Journal of Veterinary Cardiology*, 19(6), 514–522. <https://doi.org/10.1016/j.jvc.2017.09.004>
- McClure, J. J., Gaber, C. E., Watters, J. W., & Qualls, C. W. (1983). Complete transposition of the great arteries with ventricular septal defect and pulmonary stenosis in a Thoroughbred foal. *Equine Veterinary Journal*, 15(4), 377–380. <https://doi.org/10.1111/j.2042-3306.1983.tb01830.x>
- Meister, S. L., Susanna, T., Fabia, K., Christian, W., Balmelli, N., & Grau, L. (2022). *inlet univentricular heart with persistent truncus arteriosus in a Sumatran orangutan (Pongo abelii)*. (November), 1–3. <https://doi.org/10.1111/jmp.12631>
- Meurs, K. M., Miller, M. W., Hanson, C., & Honnas, C. (1997). Tricuspid valve atresia with main pulmonary artery atresia in an Arabian foal. *Equine Veterinary Journal*, 29(2), 160–162. <https://doi.org/10.1111/j.2042-3306.1997.tb01661.x>
- Mizuno, T., Mizuno, M., Harada, K., Takano, H., Shinoda, A., Takahashi, A., ... Uechi, M. (2020). Surgical correction for sinus venosus atrial septal defect with partial anomalous pulmonary venous connection in a dog. *Journal of Veterinary Cardiology*, 28, 23–30. <https://doi.org/10.1016/j.jvc.2020.01.006>
- Mohamed, T., Sato, H., Kurosawa, T., Oikawa, S., Nakade, T., & Koiwa, M. (2004). Tetralogy of fallot in a calf: Clinical, ultrasonographic, laboratory and postmortem findings. *Journal of Veterinary Medical Science*, 66(1), 73–76. <https://doi.org/10.1292/jvms.66.73>
- Monné Rodríguez, J. M., Chantrey, J., Unwin, S., & Verin, R. (2017). Cardiac Truncus Arteriosus in an Eastern Black Rhinoceros (*Diceros bicornis michaeli*). *Journal of Comparative Pathology*, 157(4), 276–279. <https://doi.org/10.1016/j.jcpa.2017.09.001>
- Morita, T., Hoshino, Y., Kobayashi, S., & Endo, K. (2022). Partial anomalous pulmonary venous connection with portosystemic shunt in a cat. *Journal of Veterinary Cardiology*, 41, 220–226. <https://doi.org/10.1016/j.jvc.2022.03.005>
- Nicolson, G., Daley, M., Makara, M., & Beijerink, N. (2015). Partial anomalous pulmonary venous connection with suspected pulmonary hypertension in a cat. *Journal of Veterinary Cardiology*, 17, S354–S359. <https://doi.org/10.1016/j.jvc.2015.05.003>
- Oguchi, Y., Matsumoto, H., Masuda, Y., Takashima, H., Takashima, K., & Yamane, Y. (1999). Balloon Dilation of Right Ventricular Outflow Tract in a Dog with Tetralogy of Fallot. *Journal of Veterinary Medical Science*, 61(9), 1067–1069. <https://doi.org/10.1292/jvms.61.1067>
- Orton, E. C., Mama, K., Hellyer, P., & Hackett, T. B. (2001). Open surgical repair of tetralogy of Fallot in dogs. *Journal of the American Veterinary Medical Association*, 219(8), 1089–1093. <https://doi.org/10.2460/javma.2001.219.1089>
- Pazzi, P., Lim, C. K., & Steyl, J. (2014). Tetralogy of Fallot and atrial septal defect in a white Bengal Tiger cub (*Panthera tigris tigris*). *Acta Veterinaria Scandinavica*, 56, 12.

- <https://doi.org/10.1186/1751-0147-56-12>
- Rao, P. S. (1980). A unified classification for tricuspid atresia. *American Heart Journal*, 99(6), 799–804. [https://doi.org/10.1016/0002-8703\(80\)90632-8](https://doi.org/10.1016/0002-8703(80)90632-8)
- Rao, P. S. (2019). Management of congenital heart disease: State of the art—part ii—cyanotic heart defects. *Children*, 6(4). <https://doi.org/10.3390/children6040054>
- Redo, S. F., & Ecker, R. R. (1963). Intrapericardial Aortico-Pulmonary Artery Shunt. *Circulation*, 28(October), 520–524. <https://doi.org/10.1161/01.CIR.28.4.520>
- Rienzo, M., Imbault, J., El Boustani, Y., Beurton, A., Carlos Sampedrano, C., Pasdois, P., ... Ouattara, A. (2020). A total closed chest sheep model of cardiogenic shock by percutaneous intracoronary ethanol injection. *Scientific Reports*, 10(1), 1–13. <https://doi.org/10.1038/s41598-020-68571-5>
- Russell, H. M., Jacobs, M. L., Anderson, R. H., Mavroudis, C., Spicer, D., Corcraïn, E., & Backer, C. L. (2011). A simplified categorization for common arterial trunk. *Journal of Thoracic and Cardiovascular Surgery*, 141(3), 645–653. <https://doi.org/10.1016/j.jtcvs.2010.08.022>
- Sagawa, K., Maughan, L., Suga, H., & Sunagawa, K. (1988). *Cardiac Contraction and the Pressure-Volume Relationship*. New York, NY: Oxford University Press.
- Sakurai, H., Sakurai, T., Ohashi, N., & Nishikawa, H. (2018). Aortic to right ventricular shunt for pulmonary atresia with intact ventricular septum and bilateral coronary ostial atresia. *Journal of Thoracic and Cardiovascular Surgery*, 156(1), e17–e20. <https://doi.org/10.1016/j.jtcvs.2018.03.047>
- Santos, A. B., Qureshi, A. M., Mery, C. M., & Shekerdemian, L. S. (2020). Aortopulmonary Shunts and Ductal Stents. In C. M. Mery, P. Bastero, S. R. Hall, & A. G. Cabrera (Eds.), *Texas Children's Hospital Handbook of Congenital Heart Disease* (pp. 282–288). Retrieved from [https://www.texaschildrens.org/sites/default/files/uploads/documents/heart/Aortopulmonary Shunts and Ductal Stents.pdf](https://www.texaschildrens.org/sites/default/files/uploads/documents/heart/Aortopulmonary%20Shunts%20and%20Ductal%20Stents.pdf)
- Schwarzwald, C., Gerspach, C., Glaus, T., Scharf, G., & Jenni, R. (2003). Persistent truncus arteriosus and patent foramen in a Simmentaler x Braunvieh calf. *Veterinary Record*, 152(11), 329–333. <https://doi.org/10.1136/vr.152.11.329>
- Serres, F., Chetboul, V., Sampedrano, C. C., Gouni, V., & Pouchelon, J. L. (2009). Ante-mortem diagnosis of persistent truncus arteriosus in an 8-year-old asymptomatic dog. *Journal of Veterinary Cardiology*, 11(1), 59–65. <https://doi.org/10.1016/j.jvc.2008.11.001>
- Shofti, R., Zaretzki, A., Cohen, E., Engel, A., & Bar-El, Y. (2004). The sheep as a model for coronary artery bypass surgery. *Laboratory Animals*, 38(2), 149–157. <https://doi.org/10.1258/002367704322968821>
- Sikkink, C. J. J. M., Zeebregts, C. J., & Reijnen, M. M. P. J. (2007). Hyaluronan-Based Antiadhesive Agents in Abdominal Surgery : Applications, Results, and Mechanisms of Action. *Surgical Technology International*, 16, 19–29.
- Sizarov, A., de Bakker, B. S., Klein, K., & Ohlerth, S. (2014). Building foundations for transcatheter intervascular anastomoses: 3D anatomy of the great vessels in large experimental animals. *Interactive Cardiovascular and Thoracic Surgery*, 19(4), 543–551. <https://doi.org/10.1093/icvts/ivu210>
- Slack, J. A., Johns, I., Van Eps, A., & Reef, V. B. (2008). Imaging diagnosis - tricuspid atresia in an alpaca. *Veterinary Radiology and Ultrasound*, 49(3), 309–312. <https://doi.org/10.1111/j.1740-8261.2008.00372.x>

- Sleeper, M. M., & Palmer, J. E. (2005). Echocardiographic diagnosis of transposition of the great arteries in a neonatal foal. *Veterinary Radiology and Ultrasound*, *46*(3), 259–262. <https://doi.org/10.1111/j.1740-8261.2005.00035.x>
- Sommer, R. J., Hijazi, Z. M., & Rhodes, J. F. (2008a). Pathophysiology of congenital heart disease in the adult: Part III: Complex congenital heart disease. *Circulation*, *117*(10), 1340–1350. <https://doi.org/10.1161/CIRCULATIONAHA.107.714428>
- Sommer, R. J., Hijazi, Z. M., & Rhodes, J. F. (2008b). Pathophysiology of congenital heart disease in the adult part I: Shunt lesions. *Circulation*, *117*(8), 1090–1099. <https://doi.org/10.1161/CIRCULATIONAHA.107.714402>
- Stephen, J. O., Abbott, J., Middleton, D. M., & Clarke, C. (2000). Persistent truncus arteriosus in a Bashkir Curly foal. *Equine Veterinary Education*, *12*(5), 251–255. <https://doi.org/10.1111/j.2042-3292.2000.tb00052.x>
- Straw, R., Aronson, E., & McCaw, D. (1985). Transposition of the great arteries in a cat. *Javma-Journal of the American Veterinary Medical Association*, *187*(6), 634–636.
- Talwar, S., Siddharth, B., Gupta, S., Bhoje, A., & Choudhary, S. (2019). Surgical repair for common arterial trunk with pulmonary dominance, hypoplasia of ascending aorta, and interrupted aortic arch. *Annals of Pediatric Cardiology*, *12*(3), 287–291. https://doi.org/10.4103/apc.APC_147_18
- Thorn, C. L., Ford, N. R., & Sleeper, M. M. (2017). Partial anomalous pulmonary venous connection in a dog. *Journal of Veterinary Cardiology*, *19*(5), 448–454. <https://doi.org/10.1016/j.jvc.2017.08.002>
- Tidholm, A. (1997). Retrospective study of congenital heart defects in 15 1 dogs. *JSAP*, *38*, 94–98.
- Unolt, M., Putotto, C., Silvestri, L. M., Marino, D., Scarabotti, A., Massaccesi, V., ... Marino, B. (2013). Transposition of great arteries: New insights into the pathogenesis. *Frontiers in Pediatrics*, *1*(JUN), 1–7. <https://doi.org/10.3389/fped.2013.00011>
- Valdeomillos, E., Jalal, Z., Metras, A., Roubertie, F., Benoist, D., Bernus, O., ... Thambo, J. B. (2019). Animal Models of Repaired Tetralogy of Fallot: Current Applications and Future Perspectives. *Canadian Journal of Cardiology*, *35*(12), 1762–1771. <https://doi.org/10.1016/j.cjca.2019.07.622>
- van der Linde-Sipman, J. S., & van den Ingh, T. (1979). Tricuspid Atresia in a foal and a lamb. *Zbl. Vet. Med.*, *26*, 239–242. <https://doi.org/10.1111/j.1439-0434.1974.tb02793.x>
- Van Der Linde, D., Konings, E. E. M., Slager, M. A., Witsenburg, M., Helbing, W. A., Takkenberg, J. J. M., & Roos-Hesselink, J. W. (2011). Birth prevalence of congenital heart disease worldwide: A systematic review and meta-analysis. *Journal of the American College of Cardiology*, *58*(21), 2241–2247. <https://doi.org/10.1016/j.jacc.2011.08.025>
- Van Praagh, R. (1976). Classification of Truncus Arteriosus Communis. *American Heart Journal*, *92*(2), 129–132. <https://doi.org/10.1067/mhj.2002.129968>
- Van Praagh, R. (2009). The First Stella Van Praagh Memorial Lecture: The History and Anatomy of Tetralogy of Fallot. *Seminars in Thoracic and Cardiovascular Surgery: Pediatric Cardiac Surgery Annual*, *12*(1), 19–38. <https://doi.org/10.1053/j.pcsu.2009.01.004>
- Vrijland, W. W., Tseng, L. N. L., Eijkman, H. J. M., Hop, W. C. J., Jakimowicz, J. J., Leguit, P., ... Jeekel, H. (2002). Fewer Intraoperative Adhesions With Use of Hyaluronic Acid – Carboxymethylcellulose Membrane. *Annals of Surgery*, *235*(2), 193–199.
- Weder, C., Ames, M., Kellihan, H., Bright, J., & Orton, C. (2016). Palliative balloon dilation of

- pulmonic stenosis in a dog with tetralogy of Fallot. *Journal of Veterinary Cardiology*, 18(3), 265–270. <https://doi.org/10.1016/j.jvc.2016.01.005>
- Wenger, S., Gull, J., Glaus, T., Blumer, S., Wimmershoff, J., Kranjc, A. H., ... Hatt, J.-M. (2010). Fallot's Tetralogy in a European Beaver (*Castor fiber*). *Journal of Zoo and Wildlife Medicine*, 41(2), 359–362.
- Yuan, S. M., & Jing, H. (2009). Palliative procedures for congenital heart defects. *Archives of Cardiovascular Diseases*, 102(6–7), 549–557. <https://doi.org/10.1016/j.acvd.2009.04.011>
- Zamora, C. S., Vitums, A., Nyrop, K. A., & Sande, R. D. (1989). Atresia of the Right Atrioventricular Orifice with Complete Transposition of the Great Arteries in a Horse. *Anatomia, Histologia, Embryologia*, 18(2), 177–182. <https://doi.org/10.1111/j.1439-0264.1989.tb00594.x>
- Zimmerman, M. S., Smith, A. G. C., Sable, C. A., Echko, M. M., Wilner, L. B., Olsen, H. E., ... Kassebaum, N. J. (2020). Global, regional, and national burden of congenital heart disease, 1990–2017: a systematic analysis for the Global Burden of Disease Study 2017. *The Lancet Child and Adolescent Health*, 4(3), 185–200. [https://doi.org/10.1016/S2352-4642\(19\)30402-X](https://doi.org/10.1016/S2352-4642(19)30402-X)

LIST OF ABBREVIATIONS

ASD: atrial septal defect
BT: Blalock-Thomas-Taussig
CHD: congenital heart disease or defect
CTA: computed tomography angiography
DORV: double-outlet right ventricle
E_A: arterial elastance
EDPVR: end-diastolic pressure volume relationship
EDV: end-diastolic volume
ESP: end-systolic pressure
ESPVR: end-systolic pressure volume relationship
ESV: end-systolic volume
MAPCAs: major aortopulmonary collateral arteries
PDA: patent ductus arteriosus
PFO: patent foramen ovale
PS: pulmonary stenosis
PTFE: polytetrafluoroethylene
PVA: pressure-volume area
RVOT: right ventricular outflow tract
TAPVC: total anomalous pulmonary venous connection
TGA: transposition of the great arteries
TOF: Tetralogy of Fallot
VSD: ventricular septal defect